

**2-D SEISMIC INTERPRETATION OF MEYAL AREA
INTEGRATED WITH PETROPHYSICAL ANALYSIS,
FACIES ANALYSIS AND COLORED INVERSION**



By

Muhammad Osman Nadeem Farooqui

BS.GEOPHYSICS

(2013-2017)

DEPARTMENT OF EARTH SCIENCES

QUAID-I-AZAM UNIVERSITY

ISLAMABAD



“In the Name of ALLAH, the Most Merciful & Mighty”

“PAY THANKS TO ALLAH EVERY MOMENT AND GO TO EXPLORE THE HIDDEN
TREASURES, ITS ALL FOR YOUR BENEFIT”

(AL-QURAN).

CERTIFICATE OF APPROVAL

This dissertation submitted by **Muhammad Osman Nadeem Farooqui**/O **Iqbal Mehmood Naseem Farooqui** is accepted in its present form by the Department of Earth Sciences, Quaid-i-Azam University Islamabad as satisfying the requirement for the award of bachelor of science degree in Geophysics.

Recommended By

Dr. Aamir Ali

(Supervisor)

Prof. Dr. Mona Lisa

(Chairperson Department of earth sciences)

External Examiner

ACKNOWLEDGEMENT

First praise is to Allah, the most Beneficent, Merciful and Almighty, on whom ultimately, we depend for sustenance and guidance. I bear witness that Holy Prophet Muhammad (PBUH) is the last messenger, whose life is perfect model for the whole mankind till the Day of Judgment. I thank Allah for giving me strength and ability to complete this study.

Foremost, I would like to express my sincere gratitude to my Supervisor **Dr.Aamir Ali** for the continuous support of my dissertation, for his patience, motivation, enthusiasm, and immense knowledge. His guidance helped me in all the time of research and writing of this dissertation. I also wish to thank the whole faculty and senior students of my department for providing me with an academic base, which has enabled me to take up this study I pay my thanks to the employees of clerical office who helped me a lot. Last but not the least I specially acknowledge the prayers and efforts of my whole family, specially my parents and my whole class fellows for their encouragement, support and sacrifices throughout the study.

Muhammad Osman Nadeem Frooqui

BS. GEOPHYSICS

(2013-2017)

Summary

Reservoir characterization using well and seismic data is a renowned technique within the context of hydrocarbon exploration. This study pertains to the interpretation of seismic lines, wire line logs and colored inversion for better visualization of important features at reservoir level.

The study area selected for this purpose is Meyal area (Upper Indus Basin) Pakistan. The area is a part of Potwar sub-basin which is known for its hydrocarbon structural traps. Datta and Patala Formations act as source rocks, Chorgali and Sakesar Formation are the two main reservoir rocks whereas Kuldana and Murree Formations act as seal/cap rocks.

The data used for this work consist of 4 seismic lines. Three of them are Dip and one Strike lines. The result suggest that study area consists of and pop-up anticlines.

Trace envelop and instantaneous phases seismic attributes are used to confirm the interpretation results and faults marking.

Facies and Petrophysical analysis of Well MYL-09 is carried out for Chorgali and Sakesar Formations in order to depict the favorable zones for hydrocarbon accumulation and their reservoir characteristics. 9% porosity and 55% hydrocarbon saturation from petrophysics indicates that the reservoir zone has effective potential.

Colored Inversion is used for developing the relationship between seismic data and well logs, to improve resolution and to calculate accurately rock properties. Very clear low impedance map of Line-07 has been achieved by inversion, shown the accuracy of this technique.

Table of Contents

CHAPTER # 1	10
INTRODUCTION	10
1.1 Reservoir Characterization:.....	11
1.2 Objective:	13
1.3 Seismic Data:	13
1.4 Base Map:	14
1.5 Introduction to Study Area:.....	15
1.6 Physiography:	16
1.7 Exploration History of Meyal Area:	17
1.8 Flow Chart:	18
CHAPTER # 2	19
GENERALGEOLOGY	19
2.1 Introduction to the Geology of Study Area:.....	20
2.2 REGIONAL SETTING:	20
2.3 Tectonic Zones of Pakistan:	22
2.4 Potwar Sub-Basin:	23
2.4.1 MAJOR FAULTS IN POTWAR BASIN:.....	24
2.4.2 MAJOR FOLDS IN POTWAR BASIN:	24
2.5 Stratigraphy of Study Area:	24
2.6 Petroleum Play:	26
2.6.1 Source Rocks:	27
2.6.2 Reservoir Rocks:	27

2.6.3 Cap Rocks:	27
CHAPTER # 3	28
3.1 Introduction of Seismic Data Interpretation:.....	29
3.2 Stratigraphically Analysis:.....	30
3.3 Structural Analysis:.....	30
3.4 Techniques for Structural Interpretation:	31
3.4.1 Time Section:	31
3.4.2 Depth Section:.....	31
3.5 Marking of Seismic Horizons:	32
3.5.1 Synthetic Seismogram:	32
3.5.2 97-MYL-05:	33
3.5.3 97-MYL-02:	34
3.5.4 97-MYL-12:	35
3.6 Fault Polygons Generation:.....	36
3.7 Observation:.....	38
3.8 Contour Maps:	38
3.8.1 Time Contour Map of Chorgali Formation:	38
3.8.2 Time Contour Map of Sakaser Limestone:	39
3.8.3 Depth Contour Map OF Chorgali Formation:.....	40
3.8.4 Depth Contour Map of Sakaser Formation:	41
3.9 Seismic Attributes:.....	43
3.9.1 Introduction:.....	43
3.9.2 Classification of Seismic Attributes:.....	43
3.9.3 Envelope of Trace (Reflection Strength / Instantaneous Amp):	44
3.9.4 INSTANTANEOUS PHASE:.....	45
CHAPTER # 4	47

PETROPHYSICAL	47
ANALYSIS:.....	47
4.1 Workflow for Petrophysical Evaluation:	48
4.2 Introduction to Petrophysics:	48
4.3 Well Logging Techniques:.....	49
4.4 Description of The Logs:	49
4.4.1 Lithology Track:	49
4.4.2 Resistivity Track:	51
4.4.3 Porosity Track:.....	52
4.5 Volume of Shale:	55
4.6 Calculation of Porosity:	55
4.7 Calculation of Resistivity of Formation Water:.....	57
4.7.1 Resistivity of Formation Water (R_w) Calculated from the SP log:.....	57
4.8 Water Saturation (S_w) Determination:	58
4.9 Hydrocarbon Saturation (S_{hc}):.....	59
4.10 Zone Marking Criteria:	59
4.11 Petrophysical interpretation of MYL-09P:	59
4.12 Interpretation for Prospect zone (3790-3850m):.....	60
CHAPTER # 5	62
FACIES ANALYSIS	62
5.1 Introduction:.....	63
5.2 Types of facies:	64
5.2.1 Sedimentary Facies:	64
5.2.2 Metamorphic facies:.....	65
5.3 Facies Analysis:	65
5.3.1 N-PHI, DT and GR cross plot:.....	65

5.3.2 GR, LLD and RHOB cross plot:	66
CHAPTER # 6.....	68
POST- STACK COLORED INVERSION	68
6.1 Introduction:.....	69
6.2 Inversion:	69
6.3 Colored Inversion:	70
6.4 Convolutional Model:	70
6.5 Acoustic Impedance:.....	71
6.6 Wavelet:	73
6.7 Procedure:	74
6.8 Wavelet Extraction:	75
6.9 Estimation of Impedence:	76
6.10 Butterworth Filter:	76
6.11 Interpretation of Inverted Section:	82
Conclusions:	83
References	84

CHAPTER # 1

INTRODUCTION

1.1 Reservoir Characterization:

If we understand our reservoir better, then we are in a better position to optimize its lifetime performance. To estimate the lifetime performance of our reservoir, we must know its characteristics, i.e. its lithology, porosity and hydrocarbon saturation, etc.

Reservoir characterization is the technique which refers to all the important information that is required for the description of reservoir in terms of its ability to store and produce the hydrocarbons. This requires complete information of reservoir geometry, fluid flow and reservoir properties (Chopra et al., 2011). It is important for quantitative estimation of rock and fluid properties, such as porosity, permeability, and hydrocarbon saturation and for EOR (Enhanced Oil Recovery), (Nanda, 2016).

Reservoir simulation requires not only geological data but also seismic, well and core data (McLean 1997).

Non-seismic methods like electromagnetic and gravity etc, have been the geophysical backbone of mineral exploration for decades. But for hydrocarbon exploration, these methods are not effective due to very low-resolution power. Here seismic technique plays the main role for hydrocarbon identification and exploration (Eaton et al., 2006). So, it has become an important tool not only for the development of oil/gas fields but also for monitoring its production (Onajite, 2014). Seismic waves are the elastic waves generated by some artificial source like vibroseis/dynamite. These waves propagate through Earth and reflected/refracted back where they are recorded by the instruments called geophones/hydrophones. The basic principle of the seismic method is that we measure the depth(s) of sub-surface boundaries, from which we can map the sub-surface geological interfaces. The depth of a reflector can be calculated by simple Equation-1.1: which is given below.

$$S = \frac{v \cdot t}{2}, \quad (1.1)$$

where, v= Velocity and t= Travel time.

There are two types of seismic methods i.e.

- Seismic Reflection method

- Seismic refraction method

The seismic reflection method is based on the study to map the subsurface geological structures, by measuring the arrival time of reflected waves. These waves reflected when the acoustic impedance changes (Kearey et al., 1984). In this method, we use body waves as they travel through Earth.

In reflection method, we also use body waves. This method is based on the study of refracted waves along the reflectors. Primarily it is applied to determine the velocity of weathered layer known as first break (Ivana et al., 2011). This velocity is useful for removing ground rolls.

The word log in oil industry means, recording of any rock characteristics with depth by using different devices in the well bore (Serra, 1988). Well log and Core analysis are one of the best geophysical techniques in terms of resolution. It is very important for the petrophysical analysis of the reservoir and for the interpolation of rock properties between different wells. It is used for the generation of the synthetic seismogram, which is used as the bench mark for the whole seismic section.

Petrophysics is the science which deals with the physical and chemical properties of porous rocks and fluids they contain. From the well logs, we use density, porosity, and resistivity of reservoir zones, from which we can find the volume of shale and fluid saturation. So petrophysics is related with wellbore for contributing reservoir characteristics (Daniel, 2003). In this technique, we quantitatively measure the porosity, permeability, capillary pressure, and saturation.

Porosity is the fundamental property of the reservoir rocks, calculated by the ratio of pore volume to the bulk volume. There is the difference between pores spaces and porosity i.e. porosity is the number (calculation), which is not visible.

Fluid saturation, such as water/hydrocarbon is the function of pore size, porosity, and capillary pressure.

Capillary pressure is directly linked to the reservoir height through the density difference of fluids involved.

Permeability is the function of porosity and pore size. While relative permeability is the function of absolute permeability and fluid saturation, and it is more important than simple permeability.

Technically and geophysically, seismic inversion is the inverse of the forward modeling that helps us to distinguish between the forward modeling and reverse modeling results. However, it must be noted that inversion and deconvolution are two different concepts.

Post-stack inversion is the technique to produce Earth's reflectivity series through acoustic impedance, this is the main objective of geophysicist (Lindseth, 1979). Generally, it is known as Acoustic Impedance Inversion, because in this we generate acoustic impedance model of Earth from the given seismic data. From this we estimate the velocity which further use for porosity and other lithological calculations. Inversion confirms the seismic results by considering well data (Ali, 2010).

1.2 Objective:

The main objective of my work is listed below.

- Structural and Stratigraphic interpretation to find the structural traps.
- To confirm structural and Stratigraphic traps by seismic attributes.
- To mark the leading zones by contouring.
- Petro-physical analysis for reservoir characterization.
- Facies analysis to support petro-physical results.
- Post-stack inversion to confirm subtle prospect zones by generation of low impedance model.

1.3 Seismic Data:

Seismic reflection data was obtained by the Department of Earth Sciences, Quaid-i-Azam University, Islamabad. This was acquired and processed by Pakistan Oil Limited (POL) in 1997. This data acquired in such a way that the trend of Dip lines is SE-NW and Strike lines is SW-NE trending. The seismic data is listed below in the Table-1.1. in this table following features are mentioned, name of lines, second column defines the nature of lines i.e. Dip or Strike, line orientation defines the geographic orientation of lines, in the last column wells are represented in front of lines at which they are present.

Table 1.1 SEISMIC DATA

Line Name	Line Nature	Line Orientation	Well
97-MYL-01	DIP	N-S	
97-MYL-02	DIP	N-S	
97-MYL-03	DIP	N-S	
97-MYL-04	DIP	N-S	
97-MYL-05	DIP	N-S	
97-MYL-06	DIP	N-S	MEYAL-08P
97-MYL-07	DIP	N-S	MEYAL-01, & 17
97-MYL-08	DIP	N-S	
97-MYL-09	DIP	N-S	MYL-1A
97-MYL-10	DIP	N-S	MYL-14
97-MYL-11	DIP	N-S	
97-MYL-12	STRIKE	E-W	MEYAL-10P & 13
97-MYL-13	STRIKE	E-W	MEYAL-16

1.4 Base Map:

The base map is the mean piece of interpretation, as it shows the spatial position of each picket seismic section. For a geophysicist, base map shows the location of seismic lines with their coordinates, well location and the points on which data is acquired. Simply it shows the dip and strike lines on which seismic survey being is carried out. Figure-1.1 shows the base map of Meyal area, lines 97-MYL-02 and 97-MYL-05 are the dip lines trending N-S while 97-MYL-12

is the strike line E-W trending. Well-10p and well-17 are represented on lines 97-MYL-05 and 97-MYL-07 respectively. Symbol N representing the northward direction. X and Y coordinates are shown, which are in meters. To compare the size of the area scale is shown on the bottom.

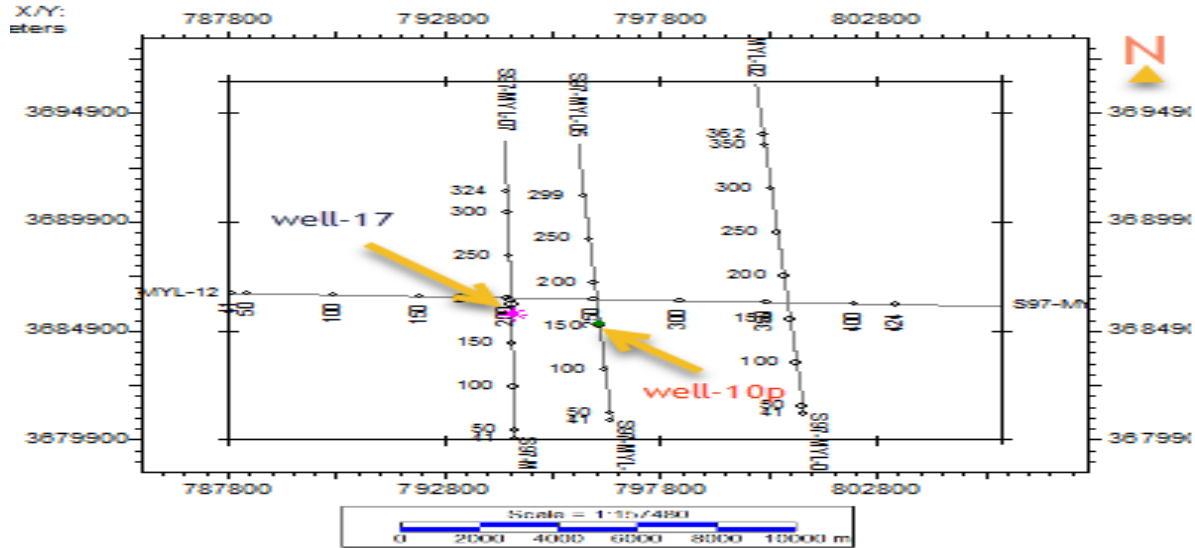


Figure 1.1: Base Map of Study Area

1.5 Introduction to Study Area:

Pakistan has the high hydrocarbon potential in its northern (Potwar-Kohat Plateau) and southern (Badin, Mari etc.) parts. The Kohat-Potwar (study area) belongs to the extra continental downward basin, represents the 48% of the world known petroleum resources (Hasany & Saleem, 2001). The predominant oil producing Potwar basin lies at the northern extremity of the upper Indus basin of Pakistan (Siddiqui and Aamir, 2006). This region is blessed with structural traps. In this region, seismic techniques are extensively used for the delineation of these structures.

From seismic we generate the model that is the representative of geological model of the earth. Limited seismic data with complex tectonic conditions create the difficulty in interpreting the seismic data (Sheriff, 1999).

My study belongs to the interpretation of given 2D seismic data of Meyal area. Meyal oilfield is situated in Pindigheb Tehsil of District Attock about $33^{\circ}17' N$ and $72^{\circ}09' E$, 23 km Northwest of Dhulian and about 92 km Southeast of Islamabad.

1.6 Physiography:

Geographic location of the Meyal is, it is the part of Potwar basin, which lies in the northern part of upper Indus basin. Kalar Kahar is in the South; Chakwal is in the East and in Talagang is in the West of Meyal. Meyal situated between latitude $33^{\circ}11'00''\text{N}$ to $33^{\circ}22'00''\text{N}$ and longitude $71^{\circ}59'00''\text{E}$ to $72^{\circ}18'00''\text{E}$. figure 1.2 shows the geographic image of my study area. Figure 1.2 shows the geographic location of Pakistan, with its neighboring countries. Meyal area is represented by red square. On the south Arabian Sea can be seen in the Figure 1.2.



Figure 1.2: Geographic Location Of Meyal (mapsofworld)

It belongs to Kohat-Potwar Fold Belt; Indus River separates the Kohat and Potwar Plateau. Kohat-Potwar Fold Belt covers the area of 36000Km^2 . This area is mostly covered by Miocene to Plesitocene sediments. Meyal is in the Southeastern part of Potwar where the structure trend is Northeast-Southwest. Lithological territories are lying unconformable over Paleozoic and the whole Mesozoic section is absent in this area.

Since Meyalis tectonically very complex, so seismic study of my area is very difficult. There is high concentration of hydrocarbon in this area, so that's why we have more than 15 oil wells in this area. Thrust related structures like Pop-up, Duplex and Anticlinal traps are common. Figure 1.3 shows the geological settings of Meyal area with Meyal Block. Figure 1.3

represents the major thrust boundaries; main geological features like anticlines, synclines, strike faults, oil fields are also represented. Scale bar is given to find the extent of any feature.

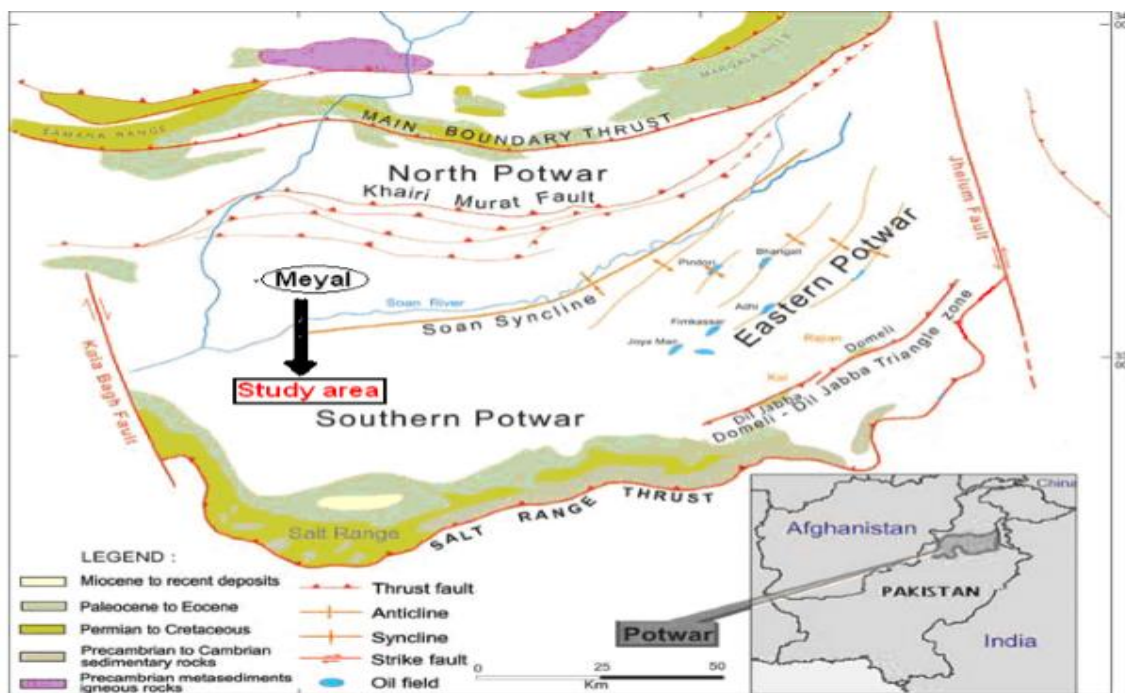


Figure 1.3: Geological Image of Upper Indus Basin (Amir et al., 2006)

1.7 Exploration History of Meyal Area:

In Pakistan first oil well was drilled in Kundal in Potwar sub-basin. The Burma Oil Company acquired first concession in 1916, they drilled three wells, but all wells were dry till 1924. Later Meyal was granted to Attock Oil Company and they drilled wells during 1924-1944.

From 1960s onward POL granted the concession of Meyal area. Seventeen wells have been drilled till now. Oil has been discovered in Eocene (Chorgali and Sakessar, Formations), Paleocene (Ranikot and Lockhart Formations), and Jurassic (Datta Formation).

POL wells number 6,8,12 and 17 are currently producing oil and gas. Well-06 drilled down to 13424 ft. Initially oil as produced from Paleocene and Jurassic, but production from Jurassic was ceased later in 1982 and currently producing from Paleocene. Well-12 is drilled up to 13622 ft in which Chorgali and Sakessar. Meyal-17 drilled up to 13660 ft and Paleocene is productive formation.

1.8 Flow Chart:

Flow chart is the pictorial representation of my project on kingdom. Flow chart is containing the steps and techniques which I have used in this project. Simplified flow chart is shown in Figure 1.4, containing steps from data loading, preparation of base map, fault polygon and horizon marking. The horizon picking is done by using synthetic seismogram which I elaborated in the chapter 6. Construction of time and depth contour maps for Chorgali and Sakessar, to shown the time and depth variation of these formation in the area. Attributes apply to confirm the fault and horizons marking. Petrophysics and facies analysis is done to confirm the pay zone and its characters by using well data. At last full stack, colored inversion is applied because inversion is new technique relative to other seismic technique and recently use in industry. Inversion is applied to confirm the pay zone with layer properties from interface properties. From the inversion, we must integrate seismic and well data. At the end of my work I summarized my conclusions and discussions.

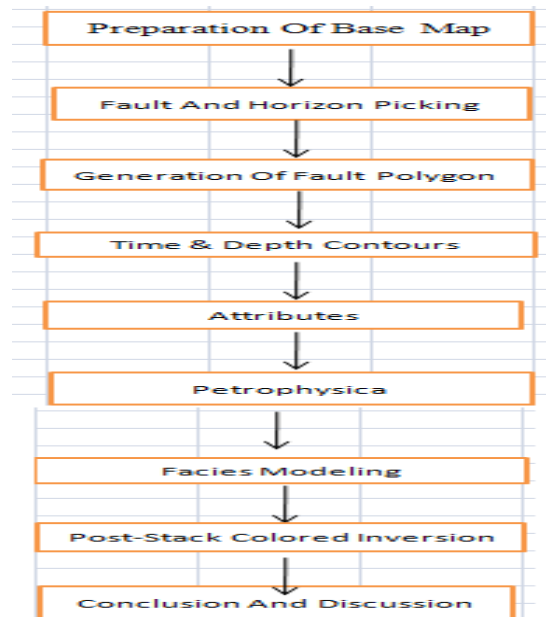


Figure 1.4: Work Flow

CHAPTER # 2

GENERAL GEOLOGY

2.1 Introduction to the Geology of Study Area:

Interpreting the Earth's history is the prime goal of geology. Information about the area geology is very important to interpret seismic data. Because seismic properties like velocity and impedance are mainly affected by the lithology and fluids (Nanda, 2016). Also, information about the position and orientation of the faults and presence of any unconformities are very important to accurately map the sub-surface.

As Mehal is situated in Upper Indus Basin, which is highly deformed area due to the presence of collision zone. Since northward movement of Indian plate produced Mariana type subduction, due to which we have Kohistan Island Arc that was fused with the plate followed by the accretion of Indian plate along the southern margin. Collision of these two plates create complex tectonic features and crystalline rocks, deformation in this area is episodic (Kazmi and Jan, 1997).

2.2 REGIONAL SETTING:

It is believed that before Paleozoic all the continents were joined together into one super giant landmass called Pangea that was surrounded by one great ocean called Panthalassa. Due to geodynamic forces, great Pangea split into two sub-continent Gondwanaland (south) and Laurasia (north) (Hallam, 1975).

The great India was the part of Gondwanaland and was rifted away from that about 130 million years (Cretaceous) ago (Johnson et al., 1976). It started movement northward and covered 5000 km distance with its greatest speed in its history. Its average speed during its movement was 16 cm/yr. Finally, Indian plate collide with Eurasian plate about 50-55 million years (Eocene) ago. Figure 2.1 shows the movement of Indian plate since Cretaceous to Eocene age, from Africa (south) to Eurasian (north) plate. This Figure 2.1 is also showing the closing of sea, that sea was called Tethys sea and the creation of Indian Ocean. Before Cretaceous Tethys sea was presented between Gondwana and Laurasia at the equator. But now on equator we have Indian plate and Indian Ocean.

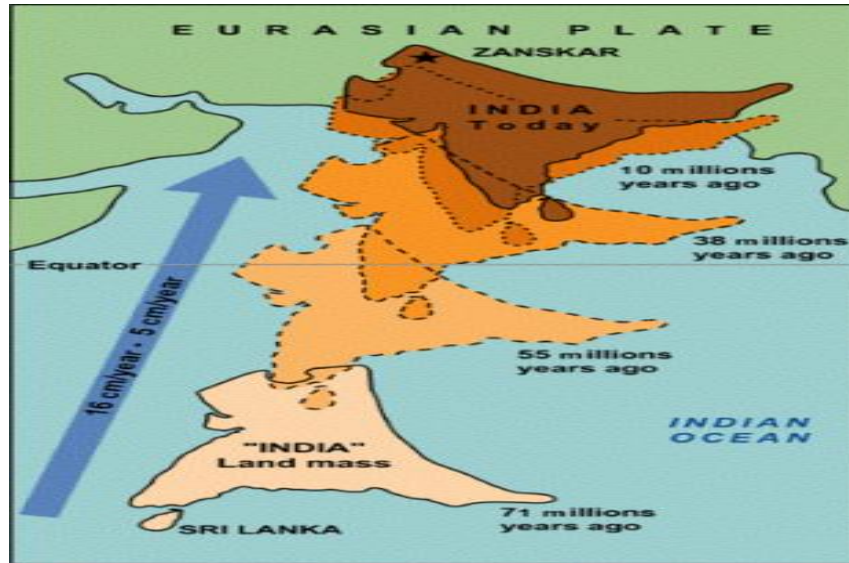


Figure 2.1: India Plate Movement (Dezes, 1999)

Due to the movement of Indian plate, Neothethys Sea was closed and Indian Ocean formed. Due to intense collision, we have Himalayas and adjacent mountain ranges. Himalayas limit in the east and west is marked by the eastern and western arc of Himalayan bends. Himalayan range is approximately 24000km long and 200-300 km wide between these bends. Approximately 600,000 sq. km in south Asia is covered by Himalayas (Kazmi and Jan, 1997). In Figure 2.2 formation of Himalayan range is shown with the subduction of Indian plate under Eurasian Plate. Tibetan Plateau is also shown whichan other feature of this subduction.

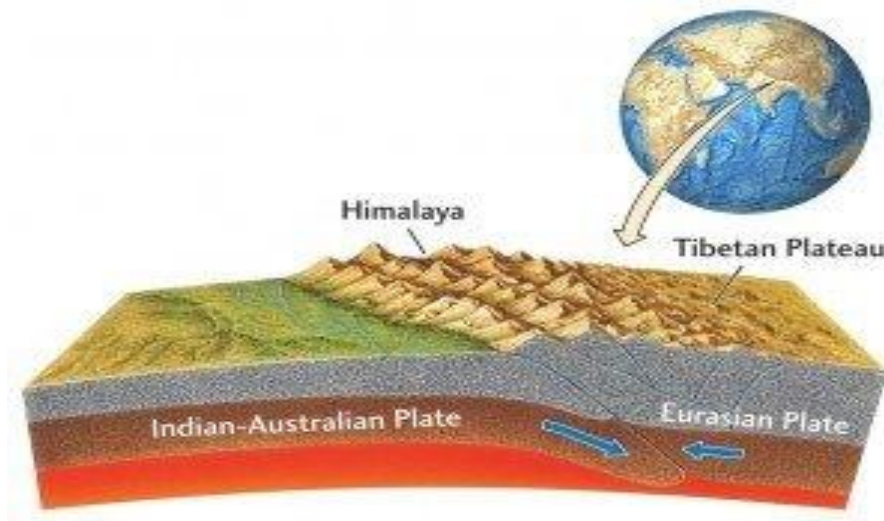


Figure 2.2 Generalized Depiction of Himalayan Collision from (FHSU, 2010)

Himalayan range is divided in to four main divisions. From N-S we have,

- Main Karakoram Thrust (MKT).
- Main Mantle Thrust (MMT).
- Main Boundary Thrust (MBT).
- Salt Range Thrust (SRT).

On the north of MKT, Karakoram and Hindukush mountain ranges are present. Kohistan Blocks on the south of MKT and on the north of MMT. Potwar Plateau present in the foreland fold, bounded on south by SRT (Pennock et al., 1989).

Pakistan situated on the northwest boundary of Indian plate.

2.3 Tectonic Zones of Pakistan:

Pakistan situated on the northwest boundary of Indian plate and can be divided in to seven tectonic zones (Kazmi and Jan, 1997).

- Indus Platform and Fore Deep.
- East Baluchistan Fold and Thrust Belt.
- Northwest Himalayan Fold and Thrust Belt.
- Kohistan-Ladakh Magmatic Arc.
- Karakoram Block.
- Kharakhorasan Flysch Basin and Makran Accretionary Zone.
- Chagai Magmatic Arc.

Figure 2.3 shows the tectonics of Upper Indus Basin, this figure shows the main thrust boundaries from Salt Range to Main Karakoram Thrust, with NPDZ. In this Figure 2.3 other features like Soan Syncline, Surghar Range etc. also shown.

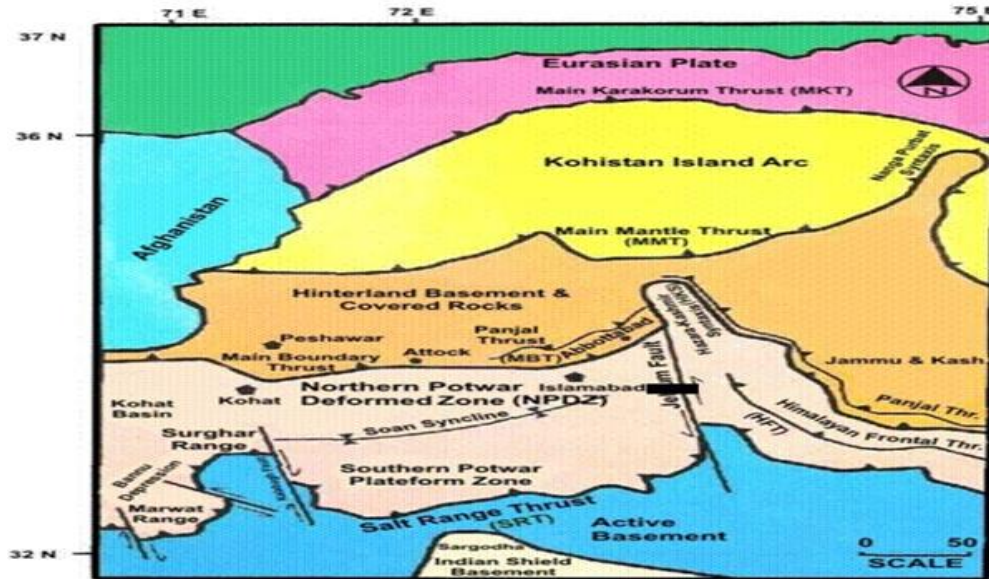


Figure 2.3 Tectonics of Upper Indus Basin (Kazmi and Jan, 1997)

2.4 Potwar Sub-Basin:

Potwar sub-basin is one of the oldest and main oil provinces in Pakistan and triangle zone plays are common in this area. It is situated in the western foothills of Himalayas in northern part of Pakistan. It includes Potwar Plateau, Salt Range and Jhelum Plain. In the Northern Potwar Deformed Zone (NPDZ) Khairi Murat Thrust-Dhurnal back thrust triangle zone while in South Potwar Platform Zone (SPPZ) Joya Mair are also well documented today. These tectonic settings contain significant amount of hydrocarbons that are being produced. Geologically this sub-basin forms the foreland part of N-W Himalayan Fold and Thrust belt. In south of Kohat sub-basin Cambrian to Pliocene age sediments are exposed, form Trans-Indus Ranges (Kadri, 1995).

We divided Potwar sub-basin into two zones based on deformation,

- North Potwar Deformed Zone.
- South Potwar Deformed Zone.

There are numerous types of folds and faults present in the Potwar sub-basin (Ahmed, 2012). Out of them are given below.

2.4.1 MAJOR FAULTS IN POTWAR BASIN:

Number of various faults and folds are present in the Potwar sub-basin, because it is situated on the southern margin of Himalayan collision zone. Some of major faults are given below,

- Khairi-Murat Fault (KMF).
- Sakhwal Fault (SF).
- Kanet Fault (KF).
- Dhurnal Back Thrust (DBT).
- Mianwali Fault (MF).
- Riwat Fault (RF).

2.4.2 MAJOR FOLDS IN POTWAR BASIN:

As this area is highly deformed so besides faults we also have several major synclines and anticlines. Major folds are given below,

- Soan Syncline.
- ChakNaurang Anticline.
- Adhi-Gungril Anticlines.
- Joya Mair Anticline
- Mahesian Anticline.
- Tanwin-Basin Anticline.
- Dhurnal Anticline.

2.5 Stratigraphy of Study Area:

To understand the general stratigraphy, we must rely on Well data. The stratigraphy of my study area is supported by the wells drilled across the Salt Range Potwar Foreland Basin (SRPFB) and the Jhelum Plain. Generalized stratigraphic column is given in the Figure 2.4; the oldest formation encounter in this area is Eocambrian Salt Range (Fatemi, 1984). Much of the thin-skinned tectonics in SRPFB are lubricated by evaporates of the Salt Range Formation (Shami and Baig, 2002).

In my study area Pre-Cambrian Salt Range Formation is overlain by Cambrian to Eocene platform sequence, like Peninsular India. Early to Middle Cambrian, Jhelum Group lies on the Salt Range Formation in SRPFB (Gee, 1934). Jhelum Group includes littoral to shallow marine Khewra and Kussak of Cambrian age. We have regional unconformity during Ordovician to Carboniferous in Upper Indus Basin, due to uplifting (Shami and Baig, 2002). So, Jhelum Group is unconformably overlain by Nilawahan Group of Permian age, includes Tobra, Dnadot, Warcha and Sardahi Formations. Zaluch Group of Late Permian age was eroded or not deposited in Upper Indus Basin, late Permian to Cretaceous rocks from west to east in this basin was eroded due to significant pre-Paleocene uplift in SRPFB.

We have thick early Paleocene to Eocene carbonate-shale sequence due to marine transgression. In this sequence, we have Locart, Patala, Sakessar and Chorgali Formations. Carbonates of this sequence provide principal oil reservoirs in this area. In SRPFB Hangu is eroded and identified on outcrop represents residual environments of deposition.

In SRPFB the Himalayan orogeny started the Eocene to Oligocene uplift and erosion (Shami and Baig, 2002). So, on the upper part of stratigraphic section of this area contain Miocene to Pleistocene non-marine molasses deposits. It includes Rawalpindi Group (Murree and Kamlial), on the top of this Group we have Siwaliks (Chinji, Nagri, DhokPathan and Soan Formations). Molasses lay on the Lower Eocene carbonates and the southern SRPFB. This molasses is generally over pressured throughout the basin. These over pressured molasses act as cap rock in the southern SRPFB, because significant part of them falls in the zone of oil window (Shami and Baig, 2002).

Figure 2.4 shows the stratigraphic chart of Potwar sub-basin, along with the regional unconformities and lithological symbols. Two time of chronostratigraphic details are shown i.e. time scale represents age as well as epoch.


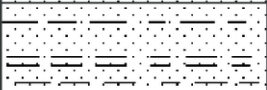
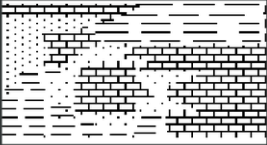
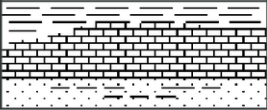

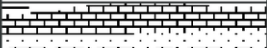

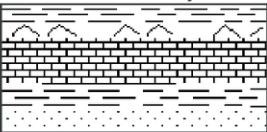
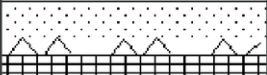
AGE / EPOCH		LITHOLOGY	FORMATION
NEOGENE	Pliocene		Nagri Chinji
	Miocene Oligocene		Kamial Murree Kohat
Oligocene		Unconformity	
PALEOGENE	Eocene		Mamikhel Chorgali # Sakesar # Nammal #
	Paleocene		Patala * # Lockhart * # Hangu * #
Mesozoic & Late Permian		Unconformity	
JURASSIC			Datta
PERMIAN	Early Permian		Chhidru Wargal Amb
			Sardhai Warcha Dandot Tobra #
Carboniferous to Ordovician		Unconformity	
CAMBRIAN TO PRE- CAMBRIAN	Cambrian		Baghanwala Jutana Kussak # Khewra * #
	Infra Cambrian		Salt Range *

Figure 2.4: Stratigraphic Column of Potwar Basin (Zaidi et al., 2012)

2.6 Petroleum Play:

The SRPFB belongs to the area of extra continental down wrap basins. This basin has complete package needed for petroleum. It has several suitable hydrocarbon accumulation features, including continental margin, thick marine sediment sequence of Eocene age, potential source, reservoir and cap rocks. The thick molasses sediments of 3047 m provide enough burial and geothermal gradient for oil formation. Average geothermal gradient is 2⁰C/100 m from oil window at the depth of 2750-5200m (Shami and Baig, 2002). Due to presence of complete package of source, reservoir and source we have Joyamair, Toot and Dhulian oilfields.

2.6.1 Source Rocks:

The gray shales of the Mianwali, Datta and Patala Formations are potential source rocks in SRPFB (Khan et al., 1986). The oil producing shales of Eocambrian Salt Range Formation include 27-36% Total Organic Content (TOC), is isolated pockets of shales, considered as source rock in this area (Shami and Baig, 2002).

2.6.2 Reservoir Rocks:

All the source, reservoir and cap rocks forming the petroleum system in Potwar are dominantly marine sediments of Paleozoic to Tertiary are exposed in Salt Range along thrust front. In NPDZ fractured carbonate rocks of Sakessar and Chorgali Formations are the major producing reservoirs. Khewra Sandstone of Cambrian and Patala Formation of Paleocene also contain good hydrocarbon reserves.

2.6.3 Cap Rocks:

Kuldana acts as cap for Chorgali and Sakessar Formations in SRPFB. Murree Formation of Pleistocene contain clay and shale also acts as a cap for Eocene reservoirs in this area as well as in Salt Range Potwar- Foreland Basin (SRPFB) where it is found to be in contact with.

CHAPTER # 3

SEISMIC

INTERPRETATION

OF MEYAL AREA

3.1 Introduction of Seismic Data Interpretation:

Interpretation of seismic is a technique by which we try to convert the whole seismic data into a structural or stratigraphically model of the earth. Since the seismic section is the replica of the geological model of the earth, by interpretation, we try to locate the anomalous zones (Nanda, 2016). Good interpretation is not the case of correctness, its consistency. For getting the accurate interpretation, not only the seismic data but also the knowledge of gravity and magnetic data, surface geology, well information with geology and physical parameters are required (Sheriff, 1999).

Seismic interpretation is the method of getting the information about the subsurface of earth. Interpretation of seismic may determine the general information about the area, locate the new prospects for drilling exploratory wells or guide the development of an already discovered field (Coffeen, 1986). According to Badley (1985), for the description of geology and hydrocarbon potential for an area we mark the reflections and unconformities on seismic sections. If the horizon of interest is not clear/prominent and it is difficult to trace it over the whole area, in this case we pick the additional horizons above and/or below the target horizon, which helps in understanding the trend and behavior of the target horizon. The final objective of interpretation is the conversion of the seismic section into the geological section, provides a somewhat realistic subsurface picture of that area, both structurally as well as stratigraphically (Badley, 1985).

Seismic interpreter ought to have a good hold in both geology and geophysics. It is the capability of an interpreter to extract the geologic significance from an aggregate of many minor observations (Sheriff, 1999).

Seismic data has been interpreted in two modes:

- The first mode is in the areas of existing well/s control, in which well data is first tied with seismic near the well location/s and then correlate with the other seismic sections.
- The second mode is in the frontier areas (no well is available), in this seismic data provides both the structural and depositional environment information.

The main purpose of interpretation is to make the reflections as clear as possible to visualize the structure and stratigraphy of the subsurface. Reflections on the seismic sections are the identification of geological boundaries where there is change in the acoustic impedance. By correlating the well with seismic we differentiate different horizons.

3.2 Stratigraphically Analysis:

To find the depositional processes and environmental settings seismic stratigraphic analysis is used, because genetically sedimentary sequence consists of concordant strata which is discordant with the above and below sequence. It is also use for the identification of formations, stratigraphic traps, and unconformities. It also helps fully to find out the major pro-gradational sedimentary sequences which are the main source of hydrocarbon generation and amplitude, velocity, frequency or the change in wave shape indicates hydrocarbon accumulation. Unconformities are marked by drainage pattern that helps to develop the depositional environment. Reef, lenses, unconformity are an example of stratigraphy traps (Sheriff, 1999).

3.3 Structural Analysis:

In Pakistan, most of the hydrocarbons are extracted from structural traps so this type of analysis is very useful in case of Pakistan. Basically, structural analysis is the study of reflector geometry based on reflection time. The main application of structural analysis of seismic section is to identify the structural traps containing hydrocarbons. Most of the structural interpretation use two-way reflection times rather than depth, and the time structural maps are constructed to display the geometry of selected reflection events. Tectonic usually governs which types of structures are formed and how these structural features are correlated with each other. Discontinue reflections clearly indicate faults and undulating reflections reveal folded beds (Sheriff, 1999).

Seismic section can predict the structure that can be extended up too few tens of kilometers. A fault having throw less than $\frac{1}{4}$ of the wavelength of seismic wave will difficult to pick in the seismic section due to tuning effect (Badley, 1985). My study area lies in the intense compressional regime, so we have usually thrust related structures i-e Pop up structure. A thrust fault develops under a high-pressure system and to develop, it required high pressure under the thrust plane. Four major faults are marked on the seismic section; indicate the complexity of the study area. The marking of these faults is based on observing the sudden change in the position

of the reflectors and distortion or disappearance of the reflection below the faults. All the faults are not extended up to the basement, that gives some indication of thin skin tectonic involvement in this study area but the normal faulting is present in the basement.

3.4 Techniques for Structural Interpretation:

Seismic sections give images of reflection arrival times. Variation along profile is called as time scanning. Structural Interpretation is done by:

1. Time Section
2. Depth Section

3.4.1 Time Section:

Time section is basically the reproduction of seismic section, Time sections have two scales one is vertical scale consisting of two-way travel time in seconds while the second is horizontal scale that consists on SP's (shot point) in meters.

3.4.2 Depth Section:

To create depth section, we need average velocity computed from CDP data. But CDP velocities are not given so I used the sonic velocities at Chorgali and Sakessar depth respectively, took the average and used in the formula 3.1. In seismic interpretation and processing, accurate measurements of seismic velocities are very important. Following method listed below is used to determine the average velocity to construct the depth section.

1. Depth Section by Dix Constant Average Velocity:

In this method, we use values of velocity and time, the depth of each interface is determined by using following Equation 3.1:

$$\text{Depth} = \frac{v \cdot t}{2}. \quad (3.1)$$

Here, t = Two-way travel time of each reflector in seconds and v = Velocity of respective reflectors

2. Depth Section by Dix Constant Average Velocity:

First average velocities from interval velocities are calculated by using Dix equation with their respective time corresponding to each CDP window. Average velocities at their respective

times under each shot point are calculated by taking arithmetic mean of interval velocities. Then we can calculate the depth of respective reflectors by using these velocities.

By using the information given in the velocity window, we can calculate the Dix average velocity. That window included information of time and interval/root mean square or normal move out velocity. Dix average velocity can be calculated by using following equation:

$$v_{int,n}^2 = (v_{rms,n}^2 * T_n - v_{rms,n-1}^2 * t_n) / (t_n - t_{n-1}). \quad (3.2)$$

where,

v_{int} = Interval velocity.

v_{rms} = Root mean square velocity.

t_n = Two-way travel time for deeper level.

t_{n-1} = Two-way travel time for shallower level.

3.5 Marking of Seismic Horizons:

The primary task of interpretation is the identification of various horizons as an interface between geological formations. For the picking of actual horizons, we required good structural as well as stratigraphic knowledge of the study area. Thus, during interpretation process, I mark both, the horizons and faults on the seismic section (McQuillin et al., 1984). I picked three horizons with the help of synthetic seismogram constructed on well-10p. The systematic procedure for the generation of synthetic will be discussed in Chapter 6. Horizons are named on basis of Well-10 tops of the well Meyal-10.

3.5.1 Synthetic Seismogram:

Synthetic seismogram is the most important feature to correlate well and seismic data at well location known as seismic to well tie. It is an artificial seismic trace established by using extracted source wavelet from the seismic data convolving with well log data. Synthetic seismogram is a useful tool for linking the sub-surface geology with seismic sections, because it can provide the direct link between observed lithologies and seismic reflection patterns (Handwerger et al., 2004). Reflection coefficients are sensitive to change in sediment impedance. Impedance is the product of compression wave velocity (V_p) and density (ρ). But it must be noted that changes in these two physical parameters may not always correspond to the

change in lithologies. Synthetic seismogram helps to identify the origin of reflectors, which are then traced laterally along the whole seismic line (Handwerger et al., 2004). Synthetic seismogram was generated on well-10p, which is shown in the Figure 3.1, which describes that, to generate synthetic seismogram we must have Time-Depth (TD) chart for that well, with sonic and density logs. In the Figure 3.1 below, after logs we have acoustic impedance column which is the product of density and velocity, which then converted into reflectivity series (R.C) by using Equation 6.1 (given in the 6th chapter). Extracted wavelet is shown in the Figure 3.1, is zero phase, by convolving this extracted wavelet with R.C (Reflectivity Coefficient) synthetic seismogram can be generated. Two columns in the Figure 3.1 are showing the seismic trace at the well location between positive and negative synthetic seismograms to confirm lithologies.

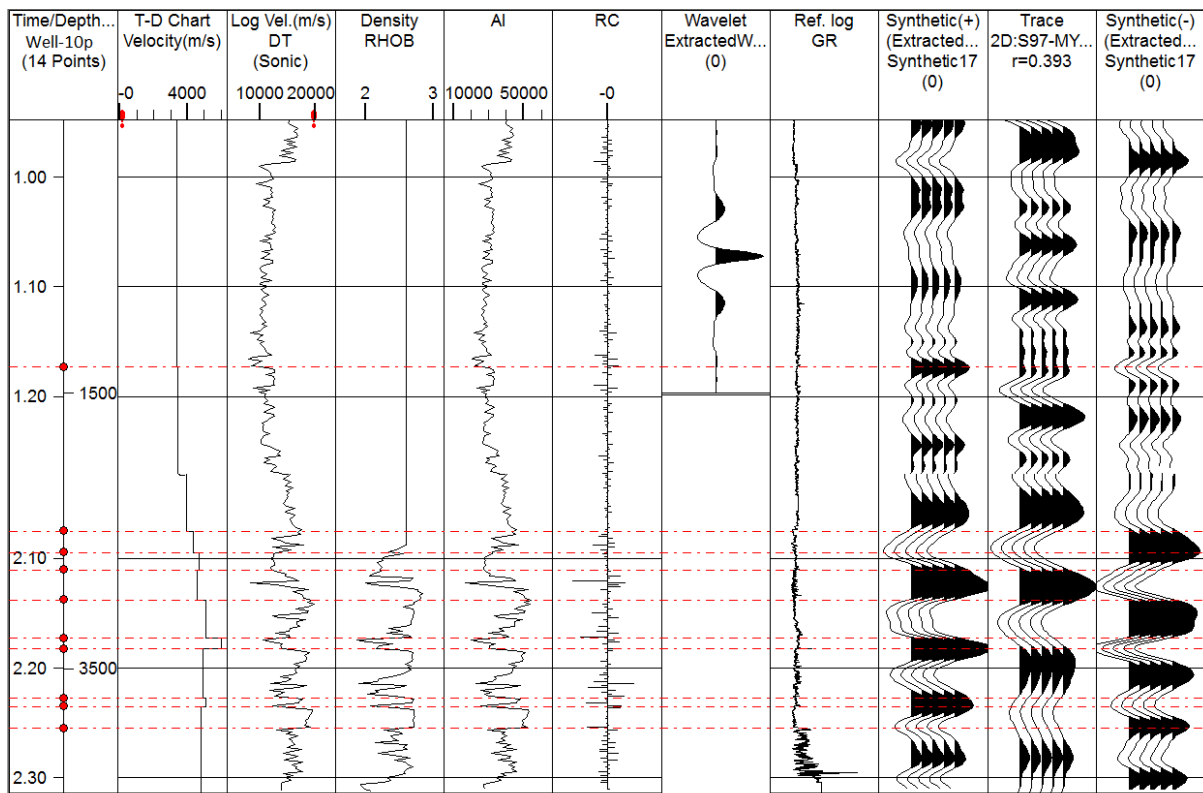


Figure 3.1: Synthetic Seismogram on well-10p

3.5.2 97-MYL-05:

This is the dip line; its trend is North-South. The interpreted seismic section of the line 97-MYL-05 is shown in the Figure 3.2; total three seismic horizons namely, Chorgali (Red),

Sakesar (Blue) and Nammal (Green) of Eocene age are marked, based on synthetic seismogram on well-10p. Along with these seismic horizons, well location and four faults are also picked. Seismic section of line 97-MYL-05 shows two pop-up structures bounded by thrust faulting. These pop-up structures are the suitable place for the accumulation of the hydrocarbons; I can say this with surety because here we have developed oil well. Thrust faulting and pop-up structures are the representation of dominant compressional regime in my study area. Relative amplitude scale bare is also shown; arrow head symbols represent short points, northward direction and two-way travel time. With the help of scale bar, we can find the Arial extent.

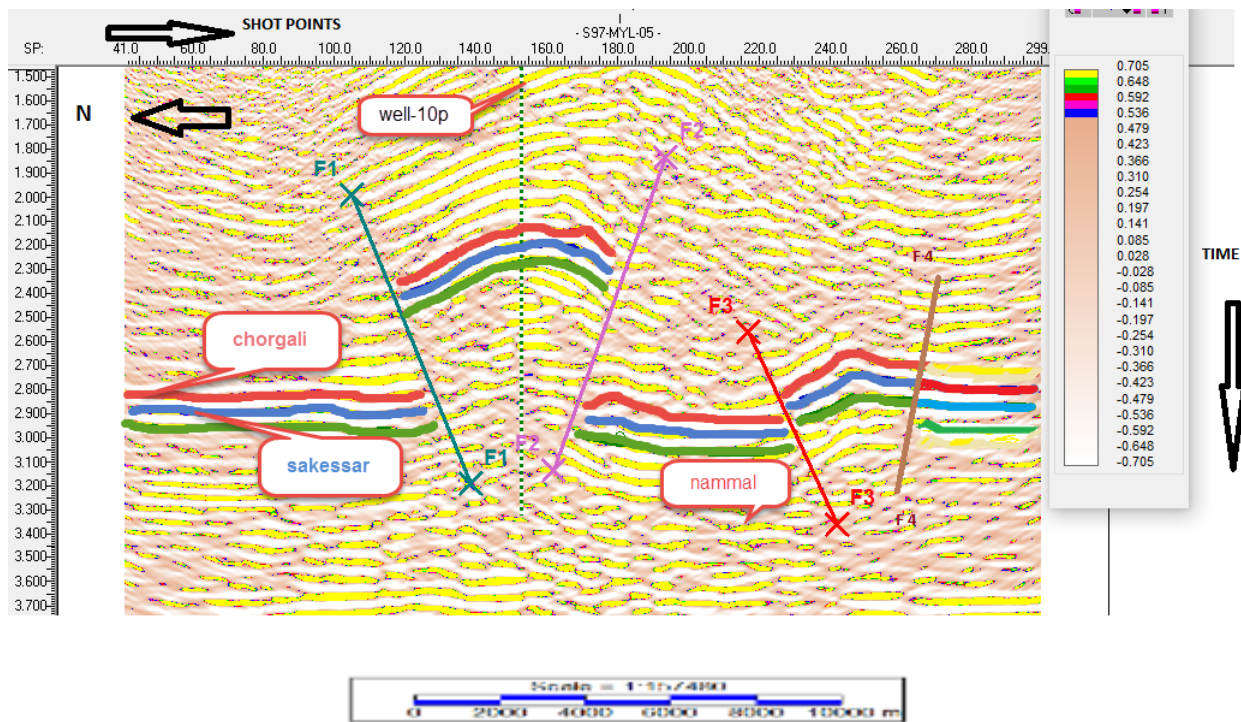


Figure 3.2: Seismic Interpretation of 97-MYL-05

3.5.3 97-MYL-02:

This is also a dip line, with the same North-South trending. The interpreted seismic section of the line 97-MYL-02 is shown in the figure 3.3 below. This line shows three same marked seismic horizons namely, Chorgali (Red), Sakessar (Blue) and Nammal (Green) of Eocene age by digitization process. Along with these seismic horizons, four faults are also picked as shown in the Figure 3.3 below. In this section, two pop-up structures bounded by thrust faulting are shown in the Figure 3.3. These pop-up structures may be the suitable place for

accumulation of hydrocarbons. For the conformation of hydrocarbon, we must apply different techniques. Thrust faulting and pop-up structures show that the study area is dominated by compressional forces. Color bar and arrow heads on the Figure 3.3 represent relative amplitude and short points, northing and two-way travel time respectively.

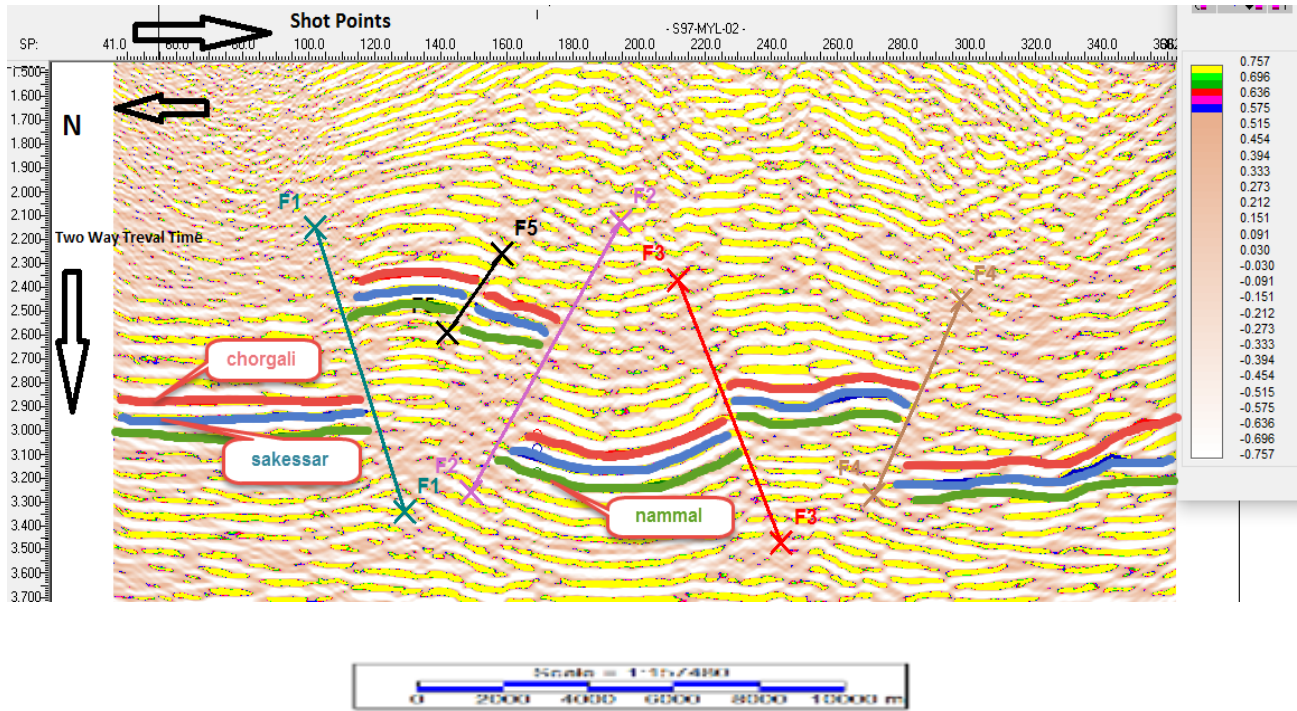


Figure 3.3: Seismic Interpretation of 97-MYL-02

3.5.4 97-MYL-12:

This is a strike line. Interpretation of seismic section of line 97-Myl-12 is shown in the Figure 3.4 below. This line is East-West trending. In this section, same three seismic horizons of Eocene age are marked namely, Chorgali (Red), Sakessar (Blue), and Nammal (Green), by digitization. All marked horizons with color bar, two-way travel time, northing, and short points with symbols are shown in Figure 3.4. In this section, we can clearly see a gentle anticlinal fold. As this is a strike line so faults are not clearly seen in this section. Color bar shown in the Figure 3.4 can be used to find the areal extent of any feature, Loke length of a reflector, fault etc.

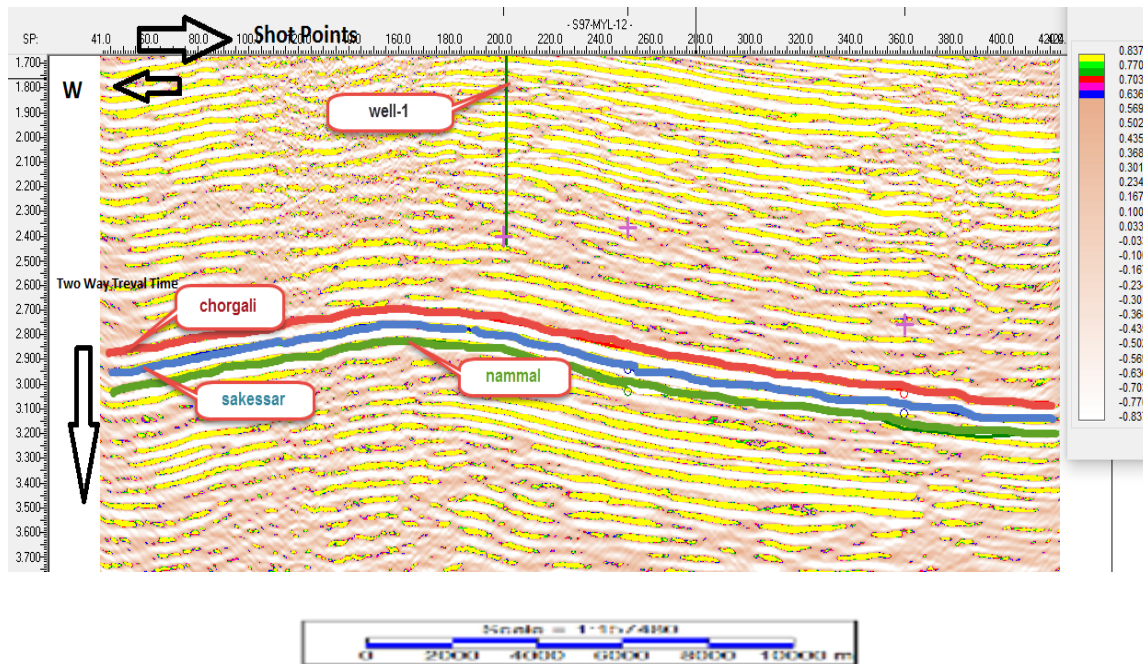


Figure 3.4: Seismic Interpretation of 97-MYL-12

3.6 Fault Polygons Generation:

Fault polygon is the technique which represents the lateral extent of dip or strike of faults having the same trend. We can identify the sub-surface discontinuities with the help of this method, by showing the displacing in contours. To generate fault polygons, it is necessary to identify the faults and their lateral extent by looking at the available seismic data. If the same fault is present on all the dip lines, then all points on the base map can be manually joined to make a polygon. Faults polygons are shown below. After the construction of fault polygons, the high and low areas on a horizon become visible. Dip directions can be shown by associated color bar or by dip symbols. It is a convention that, for reverse faults, we use triangle symbols while for normal faults we use square symbols. I have constructed fault polygons for Chorgali and Sakessar, which are oriented in E-W direction. The Figure 3.5 and Figure 3.6 show four fault polygons of Chorgali and Sakessar Formations, with X and Y coordinates in meters. With the help of color bar shown in these figures we can find the length and area of any features.

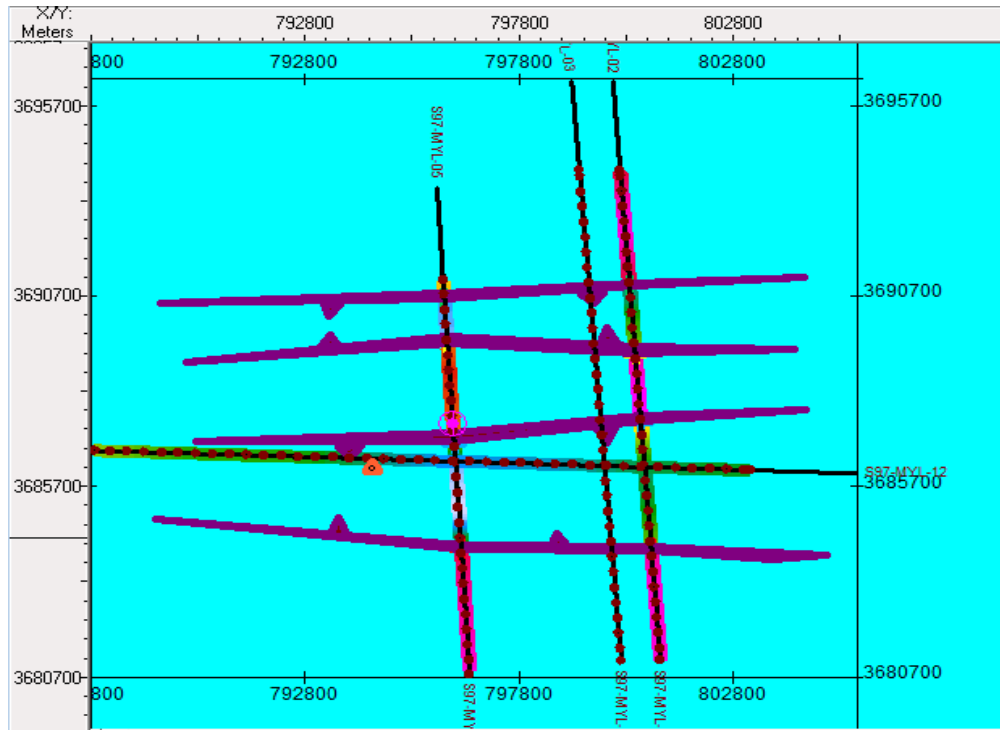


Figure 3.5: Fault Polygon of Sakessar

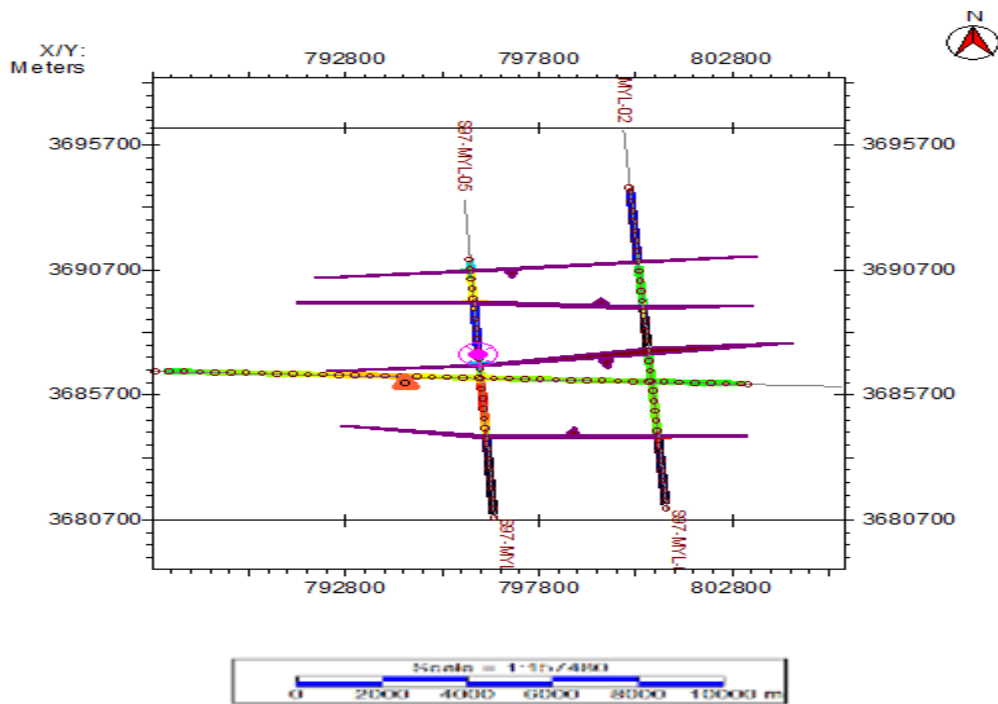


Figure 3.6: Fault Polygon of Chorgali

3.7 Observation:

I have observed East-West Trending Pop-up Structures. Marked Horizons are Chorgali, Sakasser, and Nammal formations involved in thrusting. There are Four Major Faults (F1, F2, F3, and F4) and a minor fault (F5). F1 dipping toward the north, F2 Dipping toward the south, F3 also dipping toward North, F4 Dipping toward South.F5 dipping toward the south.

3.8 Contour Maps:

Contour lines are the representation of similar event. Proficiency in contouring is the quest for a 2-D representation of a 3-D surface is a basic skill that should be in the armory of every exploration. Contours are the lines of equal time or depth wandering around the map as dictated by the data (Coffeen, 1986). Mapping is the important part of the interpretation of any data.

For the construction of a subsurface map for any geophysical data, like seismic a reference datum is very important and must be selected first. The datum may be the sea level or any other depth above or below the sea level. Occasionally, another datum is selected above the sea level to image the shallow marker on the seismic cross-section, which may have great impact on the interpretation of zone of interest (Gadallah& Fisher, 2009).

Contour line spacing is a measure of the steepness of the slope i.e. closer the spacing, steeper the slope and vice versa. Relief on the subsurface horizon shown on the structural maps with contour lines that represent two-way travel time (TWT) or equal depth below a reference datum (Gadallah& Fisher, 2009). From these contour maps, we can reveal the information about the slope, structural relief, and dip of the formation and any folding or faulting.

3.8.1 Time Contour Map of Chorgali Formation:

Chorgali formation is one of the main reservoir formations in Meyal area it belongs to marine environment. This formation has both Oil & Gas content and is mainly composed of limestone with some shaly content. Time contours of Chorgali have been shown in Figure 3.7 below, are plotted on the seismic base map along with Well locations and fault polygons. Fault polygons make pop-up structures which are suitable for hydrocarbon accumulation. Time interval is set as 20 milliseconds.

Time variation is mentioned through the color bar from (2.133 to 2.866 sec). Red to yellow colored portion (2.133 to 2.290 sec) is showing the shallowest part i.e. highest part (peak), most favorable for hydrocarbon extraction. While blue colored portion (2.693 to 2.866 sec) is showing deeper part of the formation. The pop-up structures are bounded by two major faults. In Figure 3.7 two leading zones are marked but due to limitation of data I am not sure about the second leading zone. Symbol on the right corner shows the north direction. Scale bar is also shown.

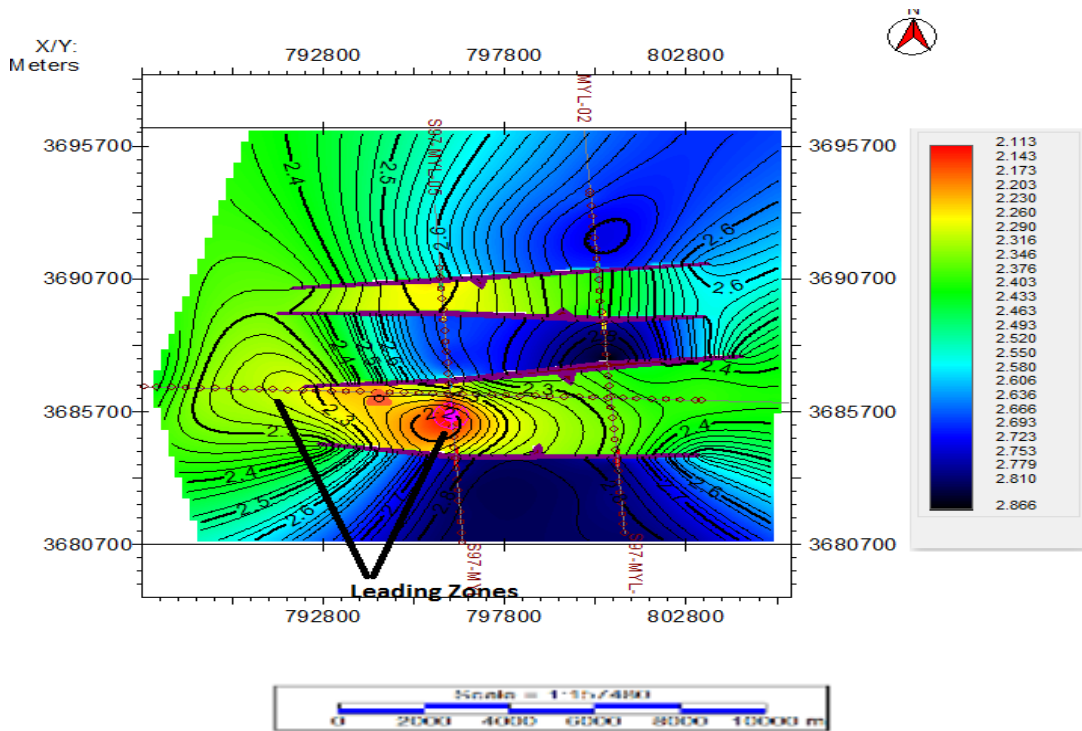


Figure 3.7: TWT Contour map for chorgali

3.8.2 Time Contour Map of Sakaser Limestone:

Sakassar formation of Eocene age is also one of the main reservoirs in Meyal area. Time contour map of Sakassar formation is shown in the Figure 3.8 below. We have same fault polygons along Chorgali and Sakassar formations which indicate the presence of the same fault on both formations. I have selected the same contour interval for both formations i.e. 20 Ms. Time variation is shown through the color bar from (2.295 to 2.951 sec). The red to yellow colored portion from (2.295 to 2.449 sec) shows the shallowest part i.e. crest (peak), may be the

most favorable part for hydrocarbon exploration. Two leading zones are marked for further calculations for development of these zones we must apply other techniques like petrophysics etc. While the blue colored portion from (2.827 to 2.951 sec) shows the deepest part of the formation. Symbol on the right corner shows the northward direction. X and Y coordinates in meters also present in the Figure 3.8.

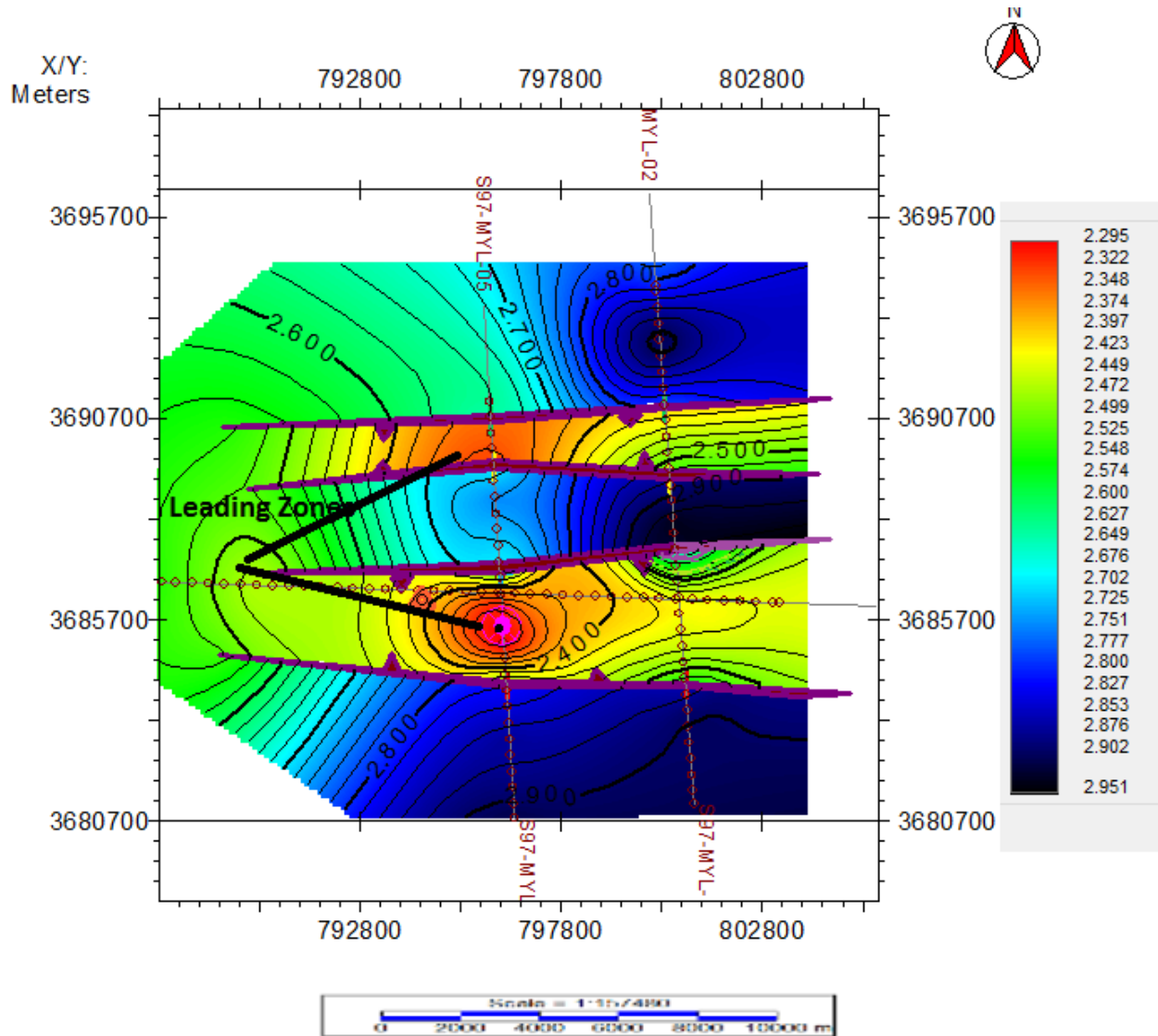


Figure 3.7: TWT Contour map for Sakessar

3.8.3 Depth Contour Map OF Chorgali Formation:

The depth contour map of Chorgali Formation is at a contour interval of 30m is shown in the Figure 3.8 below. Contour interval is 30m. For depth contouring I used kingdom built in function. I gave time from the seismic data and by using average velocity depth was

automatically calculated in the kingdom software. In this method, sub- sea was selected as reference so we have negative values with depth.

Depth ranging from 3171 to 4302 m, simply we ignore negative sign. Red to yellow colored portion (3171 to 3391 m) is showing the shallowest part (peak) while blue color (4002 to 4302 m) is showing deepest part of the formation. In Figure 3.8 three leading zones, favorable structures are marked. But I can say this with surety because low control on data.

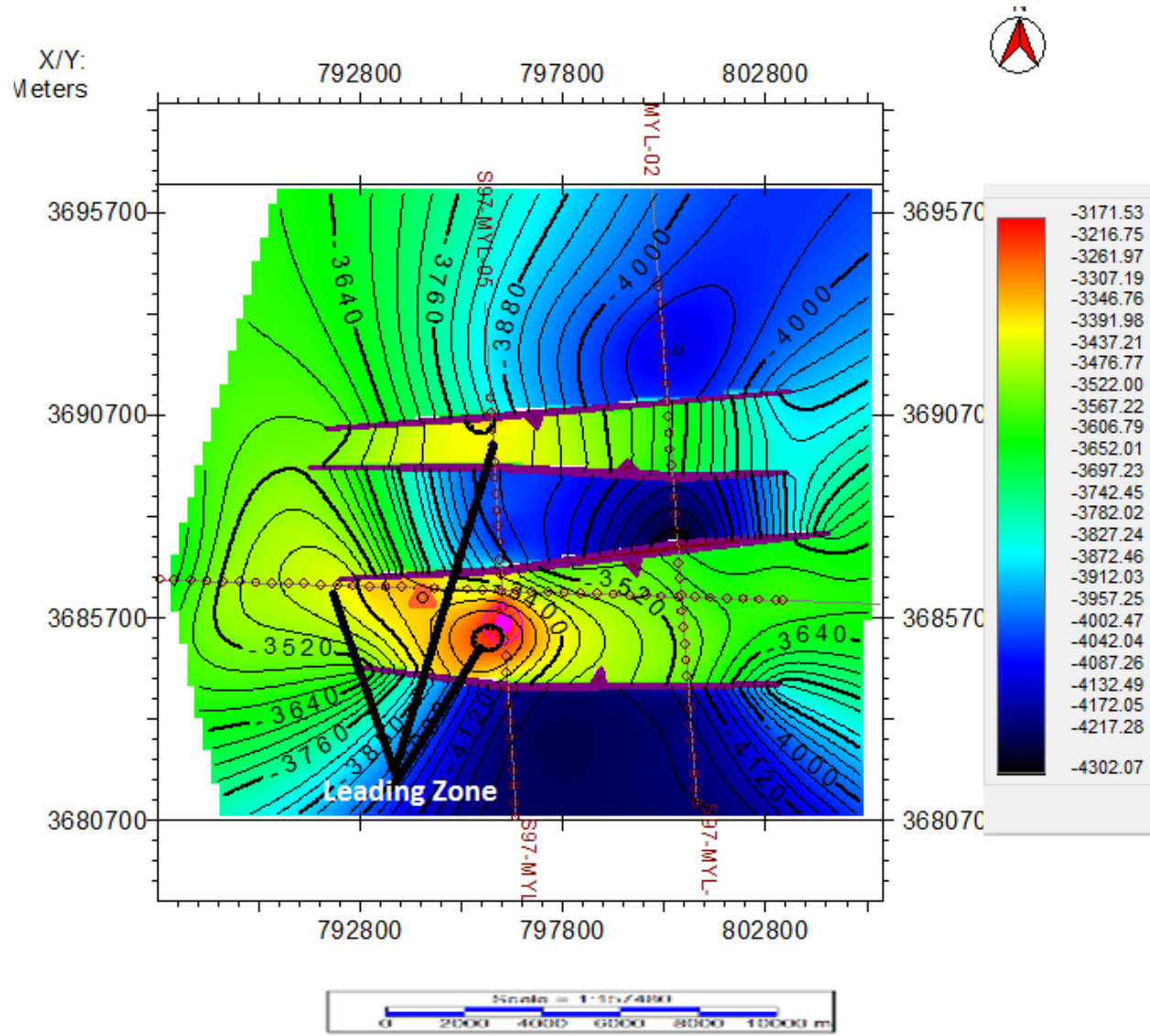


Figure 3.8: Depth contour map for Chorgali

3.8.4 Depth Contour Map of Sakasser Formation:

The depth contour map of Sakasser formation is at the contour interval of 15m shown in the Figure3.9 below. This depth contour computed differently from the previous, in this I use

replacement velocity and the time from the seismic to compute depth. Depth ranging from 2065 to 2656m. Red to Yellow colored portion from (2065 to 2200 m) shows the shallowest part (pop-up), may be the most favorable structure for hydrocarbon exploration. While the blue colored portion from (2520 to 2656m) shows the deepest part of the Sakasser formation. In this Figure 3.9, two leading zones are also shown.

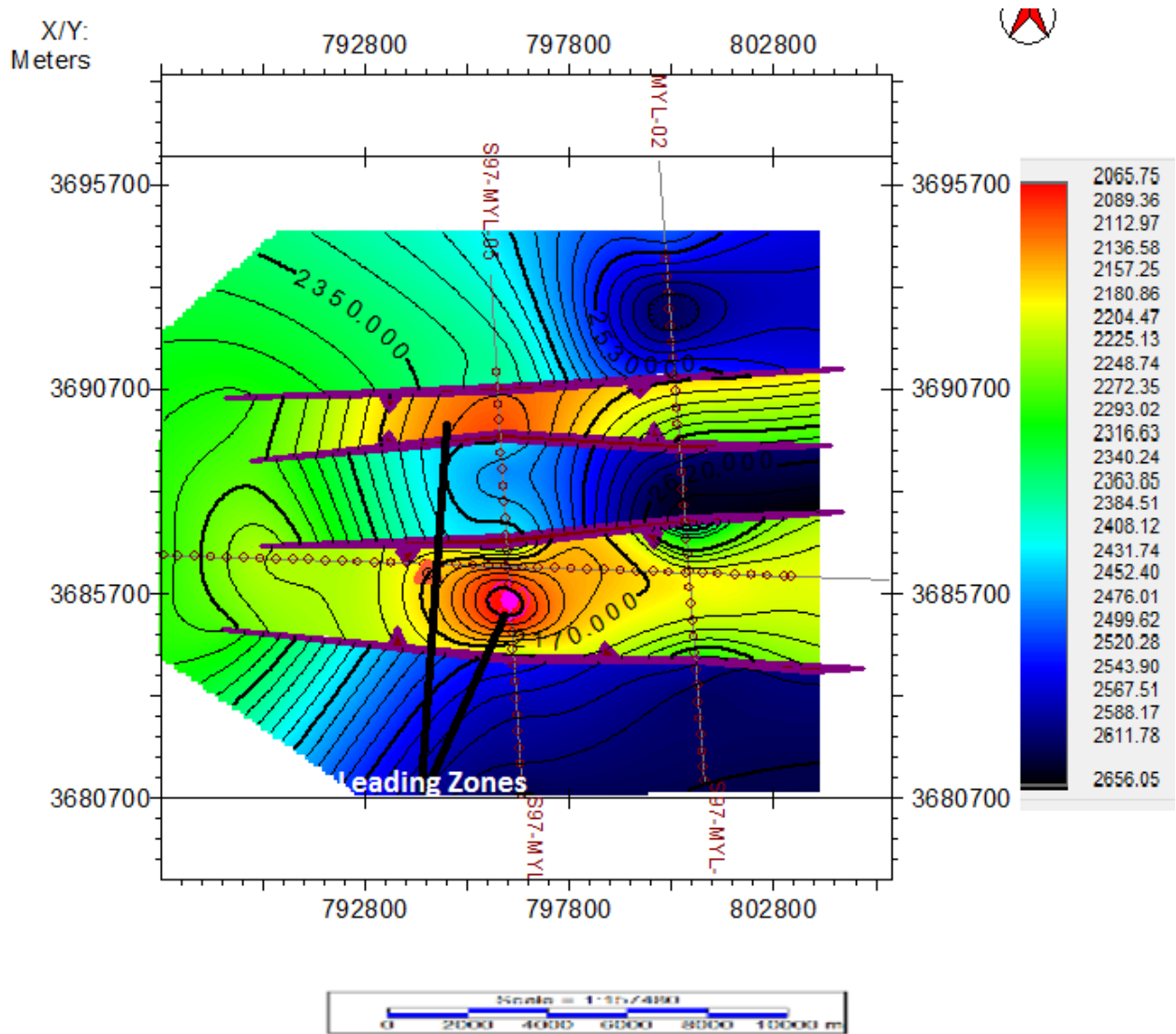


Figure 3.9: Depth contour for Sakasser

3.9 Seismic Attributes:

3.9.1 Introduction:

Attributes are inherent properties of a seismic wavelet extracted from seismic data. Subsurface geologic information is embedded in seismic wavelet; extraction of attributes with their investigation gives this embedded geologic information (Anstey, 1977). Attribute means a quality ascribed to any person or thing (Oxford), so we can say that seismic attributes are all the information acquired from seismic data, either by direct measurements or by logical or experience based reasoning.

Since 1970 seismic attributes have been used but now they become the integral part of seismic interpretation. Now a day's seismic attributes are widely used for lithological and petrophysical prediction of reservoir. To broader hydrocarbon exploration and development decision making different methodologies to extract attributes have been developed (Chopra and Marfurt, 2006).

Seismic attributes provide the qualitative information that facilitates structural and stratigraphic (channels, clinoform progradation, meanders, etc.) interpretation as well as it also provides lithology clues and fluid content estimation with a potential benefit of detailed reservoir characterization (Strecker et al., 2004).

For instant, regional and sub-seismic (subtle) faults have been marked by using seismic amplitude data but due to low resolution these faults can be interpreted more effectively with the help of seismic attributes (Gauthier & Lake, 1993). Though regional faults may be interpreted using traditional criteria (e.g. kinks, abrupt reflector cut off etc.), but subtle faults which are often of geological or exploration significance are mostly not imaged by this traditional criterion.

3.9.2 Classification of Seismic Attributes:

The study and interpretation of seismic attributes provide us with some qualitative information of the geometry and physical parameters of subsurface. It has been noted that the amplitude content of seismic data is the principal factor for the determination of physical parameters, such as acoustic impedance, reflection coefficients, velocities, absorption etc. But we define all seismically driven parameters as seismic attributes. They can be velocity, amplitude, frequency, and the rate of change of any these with respect to time or space and we have developed a classification scheme for all attributes that is based on their computational

characteristics. Principal objectives of these attributes are to provide accurate and detailed information to the interpreter on structural, stratigraphic and lithological parameters of seismic prospect (Taner, 2001). Seismic attributes can be classified in several ways, which are as follows:

a) Physical Attributes:

b) Geometric Attributes:

c) Seismic Data Domain based Classification:

- Pre-Stack Attributes
- Post-Stack Attributes

d) Computational Characteristics based Classification:

- Trace Envelope.
- Trace Envelope Derivative
- Instantaneous Frequency.
- Instantaneous Phase.

Physical attributes relate to physical qualities and quantities. Magnitude of trace envelope is proportional to acoustic impedance contrast, frequencies related to bed thickness, wave scattering and absorption. Instantaneous and average velocities directly related to rock properties. Consequently, these attributes are mostly used for lithological classification and reservoir characterization.

Geometrical attributes describe the spatial and temporal relationship of all other attributes. Lateral continuity measured by semblance. Bedding dips and curvatures give depositional information. Geometric attributes are also used for stratigraphic interpretation since they define event characteristics and their spatial relationship (Taner, 2001).

3.9.3 Envelope of Trace (Reflection Strength / Instantaneous Amp):

It represents mainly the acoustic impedance contrast, total instantaneous energy of the complex trace which is independent to phase i.e. remains always positive and calculated as the modulus of complex trace. The Hilbert transform of the real seismic trace generates the

imaginary trace, by using both real and imaginary traces the envelope trace is computed (Taner,2001).

This attribute is computed for seismic lines 97-MYL-02 and 97-MYL-05 shown in the figures below, to see major lithological changes. Even negative reflection coefficients formations such as limestone generate positive value in this attribute. Thick (yellow) indicated the maximum strength corresponding to the source, reservoir and seal rocks. It represents spatial patterns representing changes in limestone thickness and breakage due to faults.

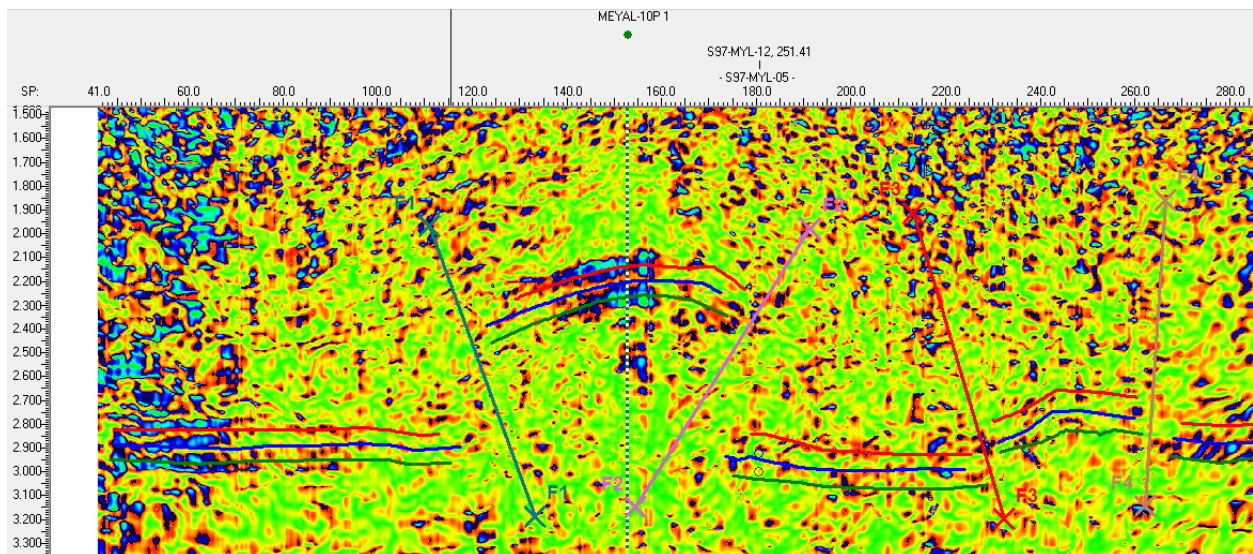


Figure 3.10: Trace envelope attribute for line 97-Myl-05

3.9.4 INSTANTANEOUS PHASE:

Phase and polarity, often considered the same, but are different attributes. An instantaneous phase section displays the phase of reflection wave form at the time corresponding to peak, trough and zero crossing. While polarity is the indicator of impedance contrast at the interface, either positive or negative (N.C Nanda, 2016). Instantaneous phase is independent to amplitude, does not vary with strong or weak reflections and lateral continuity of reflection events. So, phase correlation can be extremely useful in tracking continuity of reservoir facies where amplitude correlation does not help due to poor impedance contrasts. Instantaneous phase sections emphasize lateral discontinuities of features like faults and pinch-outs better. Important applications of this attribute are, picking up of subtle toplaps and shingle prograding clinoform, which are commonly considered as potential exploration play.

Figure 3.11 shows instantaneous phase attribute for seismic line 97-MYL-05, along the fault surfaces we get polarity reversal and this has been identified by breaking in instantaneous phase continuity. This figure confirms the fault marking.

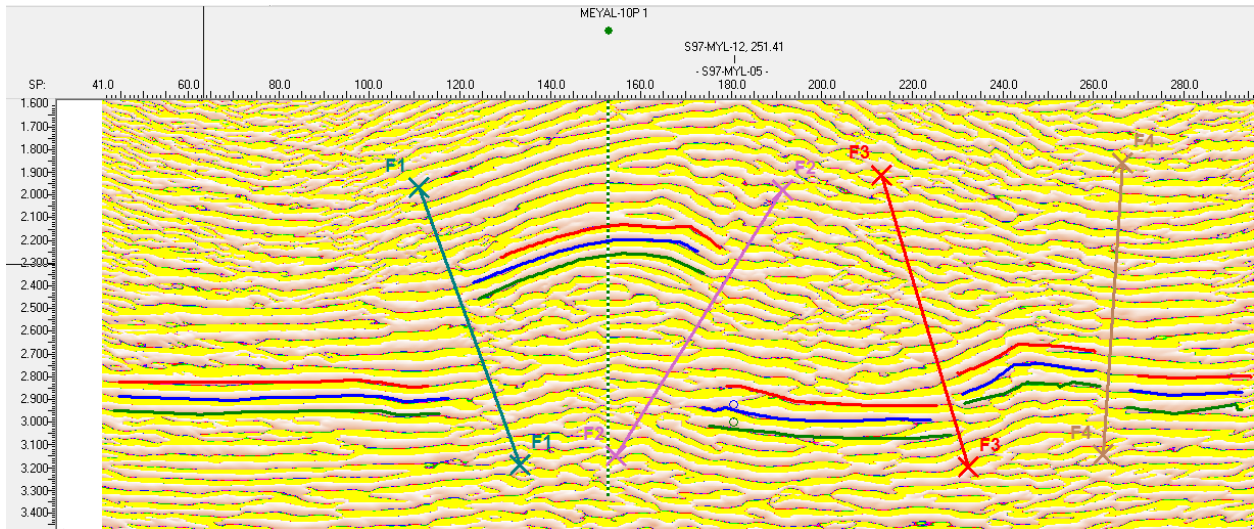


Figure 3.11: Instantaneous Phase attribute for line 97-Myl-05

CHAPTER # 4

PETROPHYSICAL ANALYSIS:

4.1 Workflow for Petrophysical Evaluation:

Figure 4.1 show the general flow for petrophysical analysis from well data loading to hydrocarbon saturation.

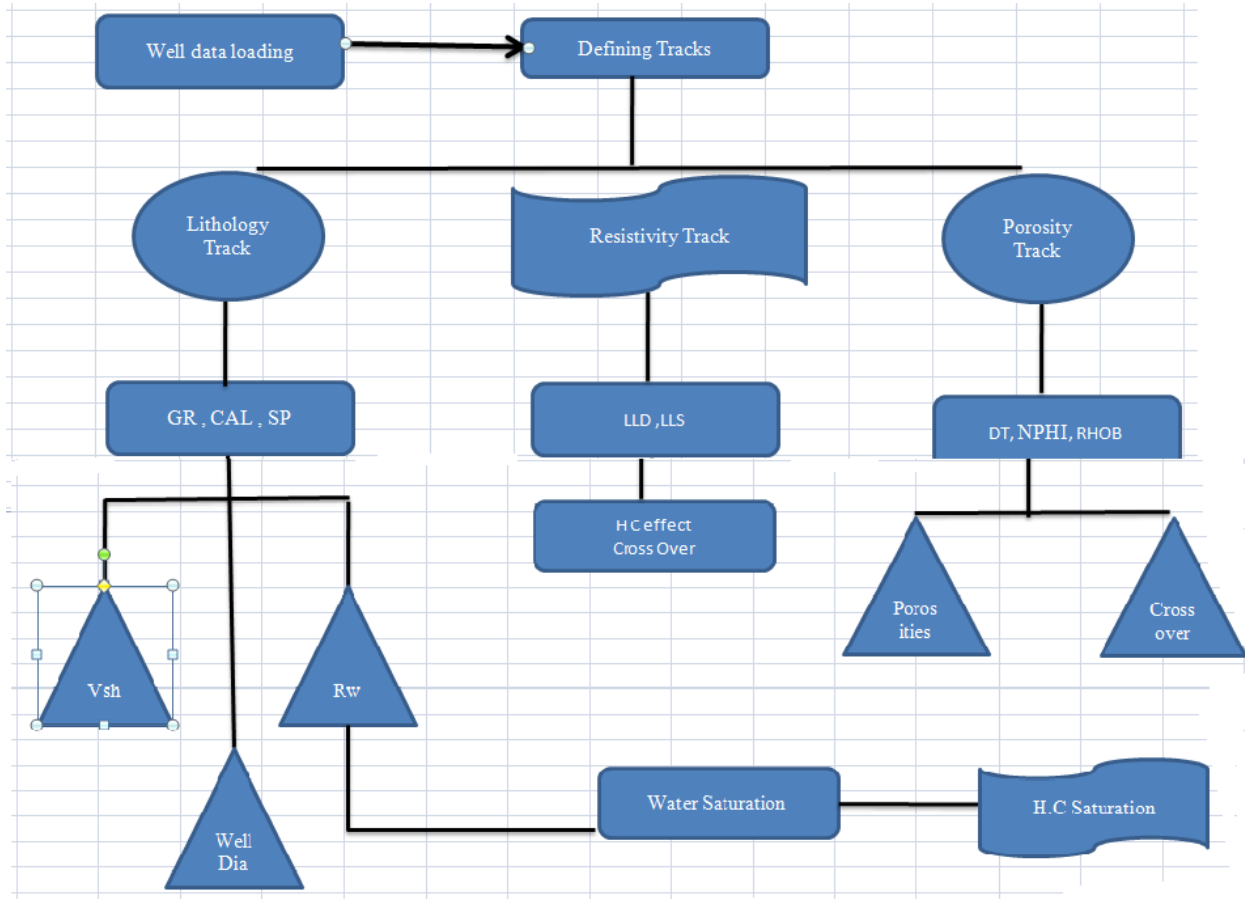


Figure 4.1: Petrophysics Flowchart

This work flow started from the well loading, then defining the tracks there are different tracks are their shown in the Figure 4.1 after defining tracks we select specific logs in specific tracks, like in lithology track we select GR, SP and CAL. After selection, the logs we compute different rock parameters like Vsh, porosity, Sw and H.C saturation.

4.2 Introduction to Petrophysics:

Petrophysics is the technique which is used for the identification of reservoir characterization. This study enables us in the identification and quantitative measurements of reservoir fluid (Ali et al., 2014).

For the marking of prospect zone, the knowledge of reservoir physical properties like the volume of shale, porosity, water, and hydrocarbon saturations are required. Geophysicists and Geologists can understand the risks and opportunities in the area by the integrated investigation of petrophysical logs. Petrophysics is the simplest technique which is used for the identification and marking of prospect zone based on visual interpretation of good measurements (Daniel, 2003).

4.3 Well Logging Techniques:

The main purpose of Well logging is to determine the various properties of different lithologies like porosity, fluid saturation etc, the actual depth of specific lithology, its thickness and interval velocity (Gendur, 2011).

In Well logging, cutting of different lithologies come up with mud filtrate. It gives the information about the type of material, type of fossil in it and gives the depositional environment information.

The petrophysical analysis are carried out by using the following wireline logs of Meyal-9

- Density Log (RHOB)
- Neutron Log (NPHI)
- Spontaneous Potential (SP)
- Resistivity Logs (LLD & LLS)
- Caliper Log
- Gamma ray (GR)

4.4 Description of The Logs:

Classifications of different logs with some short description are given as follows. We defined different tracks for different logs.

4.4.1 Lithology Track:

Lithology track also known as track 1 contains following three logs.

1. Gamma ray log
2. Spontaneous Potential log
3. Caliper log

4.4.1.1 Gamma Ray Log:

It is represented as GR log. This is one of the main logs used for the identification of lithology. This log is recorded in lithology track with Caliper and SP (Asquith and Gibson, 2004). It measures the natural radioactive contents emitting from a formation. Usually, it's used for the identification of sand and shale delineation. In common practice, sometimes non-shale content also gives the gamma rays radiation because sand- stone would contain uranium, potassium feldspar, clay fillings or rock pieces. The GR log is used in mining process, water drilling wells and by the mineral exploration companies. Every rock unit forms different spectrum as they emit different value of gamma rays. In practice, shale has highest gamma ray value than other sedimentary rocks because it emits many gamma ray radiations.

4.4.1.2 Spontaneous Potential:

Spontaneous potential (SP) records the naturally occurring potential in the well bore. In this we have two electrodes, moving and static electrodes. Moving electrode is drag into the borehole while static is on the surface as a reference. Therefore, SP curve is the record of potential difference between surface electrode and the moving electrode in the bore hole (Asquith and Gibson, 2004).

There are following utilization of this log (Daniel, 2003).

1. For the delineation of permeable zones (shale) and impermeable zone (Sand)
2. Detect boundaries of beds
3. Determine volume of shale in permeable beds
4. Determine resistivity of formation water
5. Qualitative measure of permeability

4.4.1.3 Caliper Log:

It is represented as CAL. In the exploration of hydrocarbons, it's necessary to determine the size (diameter) of the bore hole. Caliper log is used for this purpose. This log also helps us to determine the shape of bore hole as well. The presence of clay in the borehole causes swelling and caving which give the false readings, so diameter and shape should be known for the quantitative measurements of the reservoir.

4.4.2 Resistivity Track:

This is the second track. In this we run the resistivity logs (LLD and LLS). In this track, we try to find the cross-over between LLD and LLS, for the prediction of fluid presence (Gendur, 2011).

4.4.2.1 Laterolog Shallow:

It is represented as LLS. It is used for the investigation of transition zone / invaded zone. The depth of investigation is smaller than LLD. With the help of this log we can find the resistivity of flushed (R_{x0}) and transition (R_i) zones. Flushed zone occurs close to the borehole where the mud filtrate has almost completely flushed out the formation's hydrocarbons and/or water (R_w).

Whereas the transition, zone is the zone where the formation's fluids and mud filtrate are mixed. This zone occurs between flushed and uninvaded zones.

4.4.2.2 Latero log Deep:

It is represented as LLD. Deep latero log is used for the investigation of deep uninvaded zone (undisturbed zone). Uninvaded zone is the area beyond the invaded zone where the formation's fluids are uncontaminated by mud filtrate. This log is used for both saline and fresh mud. This log gives the true resistivity of the reservoir (R_t) and fluid (R_w). IT has deep penetration as compared to the (LLS). Figure 4.2 show the different zones round borehole with the resistivities. Following zones are shown in the Figure 4.2. Flushed zone is the zone in which the pore fluids are replace by mud filtrate; in this we have resistivity of mud cake. Invaded zone is that in which we have both mud and fluids in the pores of the rock, in this zone resistivity of mud filtrate can be found. Uninvaded zone is the region in which we have pure fluids are present in the pores, the true resistivity i.e. water and hydrocarbon resistivity can be found in this zone with the help of LLD log.

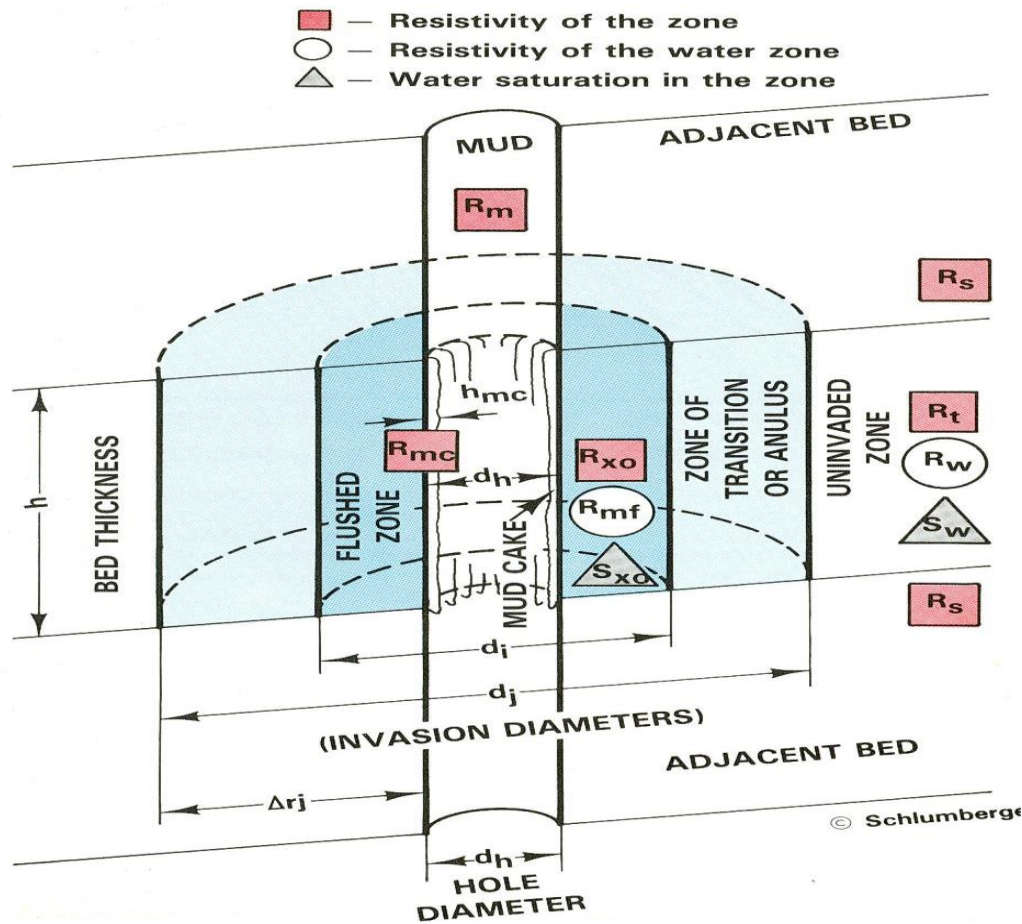


Figure 4.2 Borehole zones (Schlumberger)

4.4.3 Porosity Track:

This is the third track and in fact one of the most important track in determining the reservoir characterization. In this we use Formation density log (RHOB). Sonic log (DT) and Neutron porosity log (NPHI). In this log, we are also trying to find the cross-over between RHOB and NPHI, DT as a support. This cross-over is very important because from this we can predict the type of fluid present in the zone of interest. With the help of these logs we can find the effective porosity of the interested zone (Gendur, 2011).

4.4.3.1 Formation Density Log:

This is the log which is used for the calculation of density porosity, from which we can predict the lithological information about the interested zone. Radioactive source is used which emits gamma rays, and the amount of attenuation in the signal is dependent upon the density of

electrons in the formation. Higher the bulk density higher will be the electrons i.e. higher the attenuation and vice versa (Kearey et al., 2013).

We use following formula for the calculation of density porosity (Φ_d).

$$\Phi_d = \frac{\rho_{ma} - \rho_b}{\rho_{ma} - \rho_f}, \quad (4.1)$$

Where,

ρ_{ma} = Matrix Density

ρ_b = Formation Bulk Density

ρ_f = Fluid Density

4.4.3.2 Neutron Porosity Log:

It is represented by NPHI. This log is used for the delineation of porous formations and determination of the porosity (Kearey et al., 2013). Combination of this log with other logs such as RHOB and DT gives the accurate porosity values and lithology identification. Pores filled with water, oil or gas contains hydrogen atoms, source containing high energy neutrons when strike with hydrogen atoms in the fluid scattering occurs. Due to scattering high energy gamma rays are produced, amount of energy loss dependent relative mass of neutron and atoms present in the fluids. In case of hydrogen both contain equal mass so large amount of energy is lost and high energy gamma rays are formed. These rays are detected on the counter as the count rate. Lower the count rate higher the porosity and vice versa. According to this higher the hydrogen lower will be the count rate (Asquith and Gibson, 2004). We can find the partial concentration of hydrogen per unit mass $(C_H)_{mass}$ of a material by dividing the mass of hydrogen atoms in the material by mass of all the atoms of all elements in the material.

$$(C_H)_{mass} = \frac{n_H * A_H}{\sum_i (n_i * A_i + n_H * A_H)}, \quad (4.2)$$

Where,

n_H = Number of hydrogen atoms in a single molecule of a material.

A_H = Atomic mass of hydrogen atom.

n_i = Number of non-hydrogen atoms of i^{th} element in a single molecule of the material.

A_i = Atomic mass of non-hydrogen atoms in i^{th} element.

Partial concentration of hydrogen per unit volume $(C_H)_{\text{vol}}$ can be found by,

$$(C_H)_{\text{vol}} = \rho_b * (C_H)_{\text{mass}}, \quad (4.3)$$

4.4.3.3 Sonic log:

Also, known as acoustic log represented as DT log. It measures the travel time of elastic waves. This interval transit time is directly related with porosity of the formation (Asquith and Gibson, 2004). This log provides support RHOB and NPHI in determining the porosity and lithology. Travel time slowness (Δt), can be found by,

$$\Delta t = \frac{1}{v}. \quad (4.4)$$

Here, v = velocity

Velocity of compressional waves (P-waves) depends upon the elastic properties of the rock (matrix and fluid), so the measured of slowness varies depending upon the composition and microstructures of the matrix, type of pore fluid and porosity of the rock. Stiffer the rock more will be the velocity and vice versa. It is calculated in milliseconds per foot or millisecond per meter.

$$V \propto \frac{\text{Strength}}{\rho} \quad \text{and} \quad \Delta t \propto \frac{\rho}{\text{Strength}}$$

4.4.4 Scale of the Tracks:

Table 4.1 shows the scale range and units for different logs which I used in the petrophysics. Although the log scale range is defined but it slightly vary with area to area.

Table 4.1: Scale for Well Logs

Serial num	Log type	Range	Units
1	GR	1-150	API
2	SP	-100-100	mV
3	Caliper	4-16	Inches

4	Sonic(DT)	140-40	$\mu\text{sec/feet}$
5	RHOB	1.95-2.95	g/cm^3
6	NPHI	-0.15-0.45	PU
7	LLD/LLS	0.2-2000	Ohm-m

4.5 Volume of Shale:

Volume of shale calculated from the GR log. By using linear method, we can find IGR which is used for the calculation of V_{sh} by non-linear method. There are different formulas for non-linear method in which Stabier formula is most accurate because it gives the minimum volume of shale. Shale has maximum GR value while Carbonate and sandstone have low value of GR value, because radioactive materials are concentrated in shale. Calculation of V_{sh} is used for the delineation of reservoir and non-reservoir rock (Asquith and Gibson, 2004).

4.6 Calculation of Porosity:

- **Sonic Porosity (ϕ_s):**

Using sonic log porosity can also be easily calculated which is almost near or equal to actual porosity. The interval transit time (Δt) is dependent upon both lithology and porosity of the medium. Therefore, for formation's matrix velocity we depend upon the literature. Because velocity must be known to drive sonic porosity by the following formula given by Wyllie et al in

(1958). Sonic porosity has been calculated with help of the following the formula:

$$\phi_s = \frac{\Delta T - \Delta T_{mat}}{\Delta T_f - \Delta T_{mat}} \quad (4.5)$$

Here, ϕ_s =Sonic porosity $\mu\text{s/ft.}$, ΔT =Log response, ΔT_{mat} = Transit time in matrix, ΔT_f = Transit time in fluids

Porosity estimation for consolidated sandstone and limestone we use Wyllie formula. According to Wyllie's formula, interval transit time (ΔT) increases due to the presence of

hydrocarbon. To correct this suggestion following empirical correction is used for hydrocarbon effect.

For Gas,

$$\phi = \phi_s * 0.7$$

For Oil,

$$\phi = \phi_s * 0.9$$

- **Density Porosity (ϕ_D):**

Density porosity can be estimated by using following formula.

$$\phi_D = \frac{\rho_m - \rho_b}{\rho_m - \rho_f}, \quad (4.6)$$

where,

$$\rho_m = 2.71 \text{ gm/cm}^3$$

$$\rho_f = 1 \text{ gm/cm}^3$$

ρ_b = log Response in zone of interest

Average range of density porosity,

Chorgali = 9% to 11%

- **Total porosity (ϕ_T):**

Also, called average porosity. For the estimation of total porosity, we use following formula:

$$\phi_T = \frac{\phi_s + \phi_D}{2}, \quad (4.7)$$

where, ϕ_T = Total porosity, ϕ_s = Sonic porosity, ϕ_D = Density porosity

Average range of total porosity,

Chorgali = 10% to 12%

- **Effective Porosity (ϕ_E):**

Effected porosity can be calculated by removing the effect of shale volume (V_{sh}) from the total porosity. So, we use following formula:

$$\phi_E = \phi_T * (1 - V_{sh}), \quad (4.8)$$

Average range of effective porosity,

Chorgali = 9% to 12%

4.7 Calculation of Resistivity of Formation Water:

With the help of following methods, we can find the resistivity of formation,

- SP LOG method
- Formation water laboratory analysis
- Regional study work

4.7.1 Resistivity of Formation Water (R_w) Calculated from the SP log:

SP log integrated with Electric Induction log is used for finding the resistivity of formation water (R_w) in following way,

First, determine the formation temperature to correct the resistivity of mud filtrate (R_{mf}) and drilling mud (R_m). R_m is obtained from log header. Then, SP is corrected to Static Spontaneous Potential (SSP) to minimize the bed thickness effect. SP represents the maximum value of formation, if unaffected by bed thickness.

For determining SSP we need, bed thickness, resistivity from shallow-reading resistivity tool (R_t) and the resistivity of drilling mud (R_m) at formation temperature.

Once SSP is calculated, it is used to obtain the value for $\frac{R_{mf}}{R_{we}}$ ratio. Equivalent resistivity (R_{we}) is obtained by $R_{mf} / (R_{mf}/R_{we})$.

R_{we} is then corrected to R_w , for average deviation from sodium chloride (NaCl) solutions, and for influence of formation temperature.

It is important to note that, normally SP curve has less deflection in hydrocarbon bearing zones and this is called “Hydrocarbon Suppression”. Results are too high for R_w calculated from SSP. Therefore, use SP curve whenever possible opposite to known water bearing zones.

But rather than using harts we use mathematical formulas, which are listed below.

Mathematical Calculation of R_w from SSP (modified after Bateman & Konen, 1977).

$$R_{mf} \text{ at } 75^{\circ}\text{F} = \frac{R_{mf \text{ temp}} * (\text{temp} + 6.77)}{81.77}, \quad (4.9)$$

Correction of to R_{mf} 75°F

$$K = 60 + (0.133 * T_f), \quad (4.10)$$

R_{mfe} formula, if R_{mf} at 75°F < 0.1

$$R_{mfe} = \frac{(146 * R_{mf} - 5)}{(337 * R_{mf} + 77)}, \quad (4.11)$$

R_{mfe} formula, if R_{mf} at 75°F > 0.1

$$R_{mfe} = 0.85 * R_{mf}, \quad (4.12)$$

$$R_{we} = R_{mfe} / R_{mf} / R_{we}, \quad (4.13)$$

$$R_{mfe} / R_{we} = 10^{-SSP/K}, \quad (4.14)$$

R_w at 75°F formula, if R_{we} < 0.12

$$R_w \text{ at } 75^\circ\text{F} = \frac{(77 * R_{we} + 5)}{(146 - 337 * R_{we})}, \quad (4.15)$$

R_w at 75°F formula, if R_{we} > 0.12

$$R_w \text{ at } 75^\circ\text{F} = - [0.58 - 10^{(0.69 * R_{we} - 0.24)}], \quad (4.16)$$

$$R_w \text{ at formation temperature} = \frac{R_w \text{ at } 75^\circ\text{F} * 81.77}{T_f + 6.77}, \quad (4.17)$$

$$R_{mfe} = R_{mf} \text{ at a temperature other than } 75^\circ\text{F}$$

where, R_{mfe} = Equivalent resistivity, R_{mf} = Resistivity of mud filtrate, R_w = Resistivity of water, R_{we} = Resistivity of equivalent of wate.

Using above mentioned method R_w is calculated.

4.8 Water Saturation (S_w) Determination:

Water saturation has been calculated with help of the Archie's Equation:

$$S_w = \sqrt{\left(\frac{a}{\phi^m}\right) * \left(\frac{R_w}{R_{wt}}\right)}. \quad (4.18)$$

Here, S_w = water saturation, R_w = water resistivity (formation), ϕ^m = effective porosity, M (cementation factor) = 2, a (constant) = 1, R_t = log response (LLD), R_w has been calculated with help of the following formula:

$$R_w = \phi^2 * R_t, \quad (4.19)$$

where, ϕ = porosity in clean zone, R_t = Observed LLD curve in clean zone.

Average S_w in Chorgali formation = 38-40%.

4.9 Hydrocarbon Saturation (S_{hc}):

Hydrocarbon saturation is most important calculation in reservoir characterization. S_{hc} must be greater than 50% for productive reservoir. It can be calculated by following formula,

$$S_{hc} = 1 - S_w, \quad (4.20)$$

Average S_{hc} in Chorgali = 58-60%.

4.10 Zone Marking Criteria:

Based on one log we cannot identify the zone of interest we correlate the results of different logs and get results which give the identification of productive zone. We marked the zone of interest by following criteria,

- Low GR value is the identification of clean lithology i.e sand or limestone.
- Cross-over between LLD and LLS, indicates the presence of high resistive fluid i.e. oil/gas.
- Cross-over between NPHI and RHOB is one of the clear identification of hydrocarbon bearing zone.
- Effective (ϕ_E) and average/total (ϕ_T) porosities greater than 8.5%.
- Greater hydrocarbon saturation (S_{hc}) than water saturation (S_w).

Hence by considering all these results we can assure that our marked zones are productive.

4.11 Petrophysical interpretation of MYL-09P:

Well MYL-09P has been used for petrophysical analysis I have used MYL-09P instead of MYL-10P because we have data limitation for MYL-10P i.e. we do not have NPHI and

RHOB logs which are the one of the main logs in petrophysics. We can correlate these two wells as they are at the same line i.e. on line 97-MYL-05. Based on different behavior of different log curves, I concluded the petrophysics analysis. GR as a first indicator of lithology, suggests where the shale may be predictable. As higher the GR value higher will be the percentage of shale. Due to this reason, shale free zone (clean zone) is defined easily.

So, zone having low volume of shale may be the place of hydrocarbon accumulation. But to confirm the hydrocarbon presence we must integrate other logs too that give the comprehensive report about hydrocarbon and water saturation present in that zone.

Principal use of resistivity log is to detect and quantify hydrocarbon. So, resistivity logs are used to find the volume of oil/gas in a reservoir, in terms of petrophysics resistivity logs are used for the calculation of water saturation (S_w). If S_w is less than 100%; then hydrocarbon is present. Higher resistivity values usually indicate the presence of hydrocarbons or fresh water. If the separation between LLD and LLS is quite recordable in a zone, then the zone is hydrocarbon bearing zone. This separation occurs due to the change in LLD values i.e. in true resistivity and the value of LLD is much higher in case of oil/gas. Finally, the type of fluid is confirmed by the cross over between NPHI and RHOB, in case of oil density porosity and neutron porosity decreases this decrease is more significant for gas. If the decrease is not significant it represents presence of water. Density in my study area mainly varies from 2 to 2.7 g/cm³.

4.12 Interpretation for Prospect zone (3790-3850m):

In Myl-09P depth range of A interval varies from (3790-3850) m. It consists of interbedded shale and limestone. This zone contains 20% V_{sh} and 38-48% S_w . A prominent zone is marked through the well section in Figure 4.3, where high net pay is expected. A prominent LLD and LLS separation is observed. This zone bears relatively low values of GR, resistivity and high porosity the detail of this zone is shown below. Figure 4.3, represents my petrophysical results on well-9p. In Figure 4.3, red window is selected for promising zone, different color schemes are shown to delineate different logs. I use shading for the better visualization of crossovers between LLD and LLS, and RHOB and NPHI.

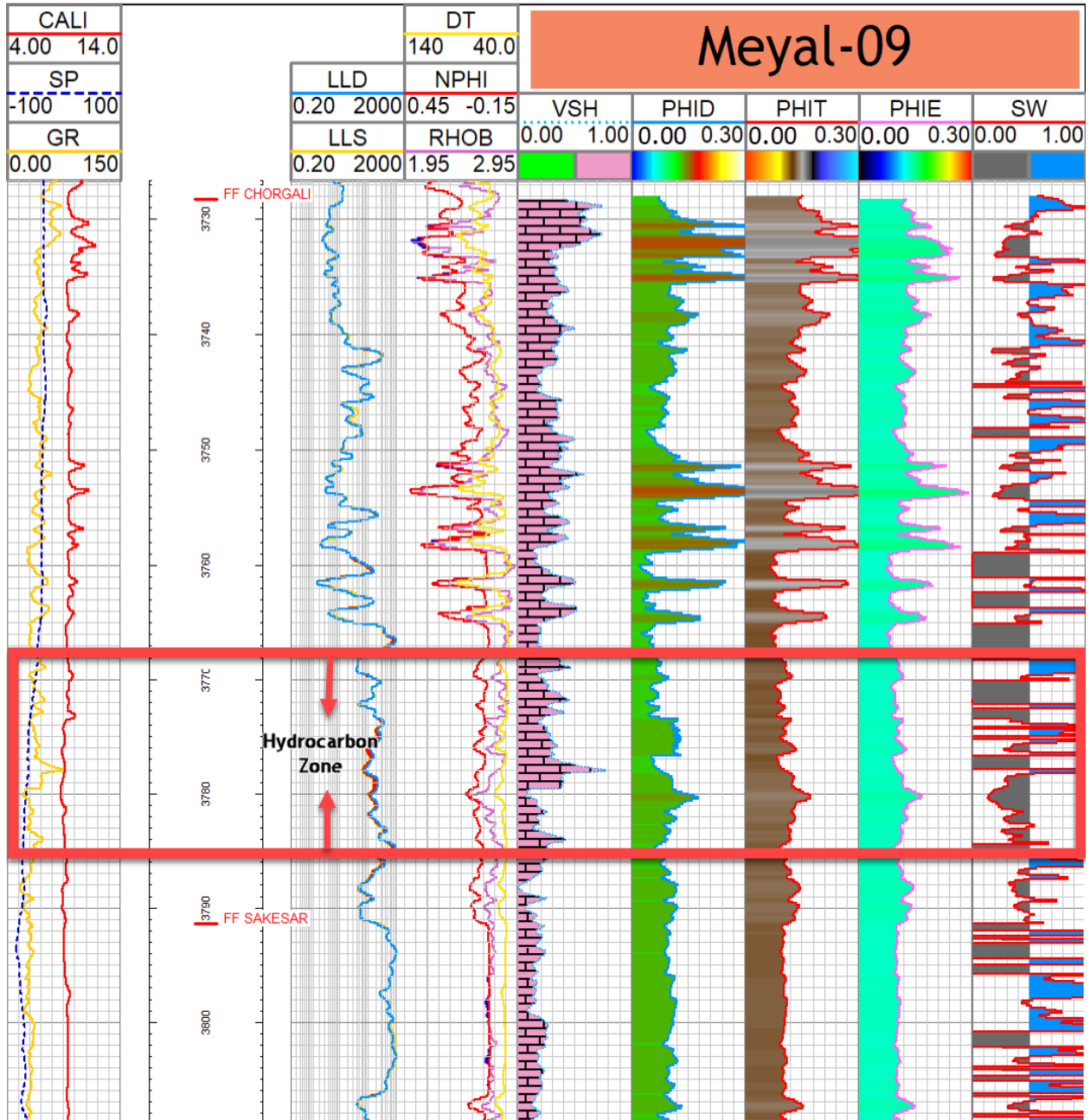


Figure 4.3: Petrophysical interpretation of Meyal-09 with prospect hydrocarbon zone

CHAPTER # 5

FACIES ANALYSIS

5.1 Introduction:

Per Moore (1949), facies is broken parts of different nature, which belong to any genetically related body of sedimentary deposits. Moore emphasizes that facies are different aspects of stratigraphic units which have mutually space distribution and clarifies the relationship between facies and lithotopes (Mutti and Lucchi, 1978).

In geology, the word facies are related to the rock with specific characteristics which are distinguished from the other rocks (Ravia et al., 2010).

Facies are the different rock unit which forms under specific condition, so it represents specific depositional environment. Depositional environment is the specific type of place where the facies are deposited, such as Glacier, Sea bottom, Delta, Glaciers etc. The term facies were introduced by the Swiss geologist AmanzGressly in 1838. Figure 5.1 shows the different seismic facies with relevant depositional environment, legends are given. Four types of facies are given in Figure 5.1, glacier, narrow channels, broad complex channels and incised valley. One type of sediments can be formed in more than one environments e.g. sand can be found in narrow channels, in complex channels and in incised valley.

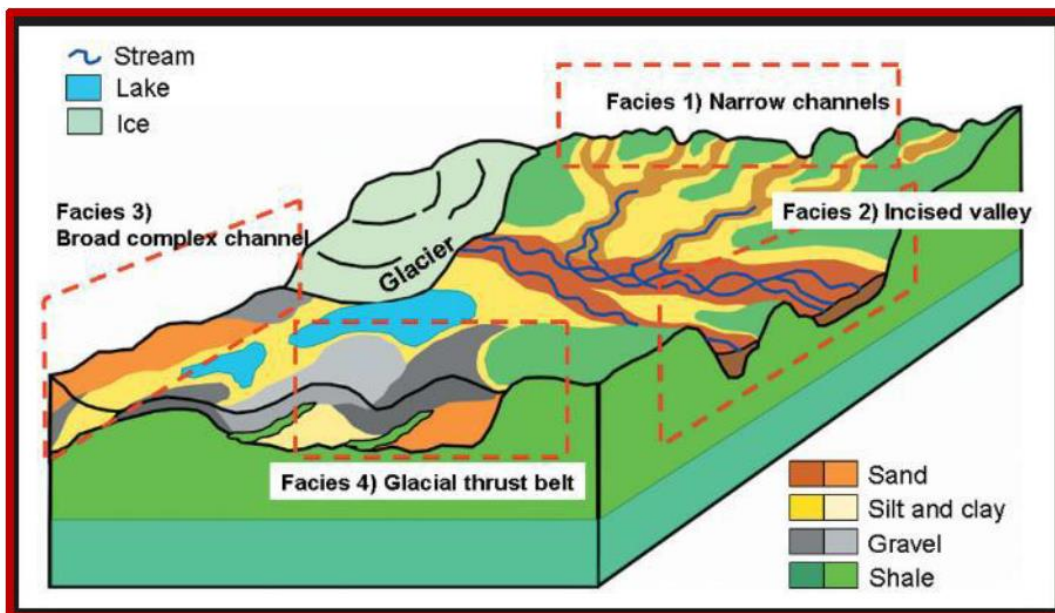


Figure 5.1: Different Environment with different facies

5.2 Types of facies:

There are different types of facies are there. In the following section, sedimentary and metamorphic facies are defined.

5.2.1 Sedimentary Facies:

Sedimentary facies are the sediments of considerably different from adjacent sediments deposited in different depositional environment. Generally, geologists distinguish facies by the aspect of the rock or sediment being studied. Facies based on petrological characters (such as grain size and mineralogy) are called lithofacies, whereas facies based on fossil content are called biofacies (Ravia et al., 2010). The characteristics of the rock unit come from the depositional environment and from the original composition. The shallow marine lagoon was the depositional environment of Chorgali and Sakessar. Figure 5.2 shows sedimentary facies i.e. on the top we have shale, below it we have sand, then limestone and red color in the bottom show the marl.



Figure 5.2: Sediment deposited in a different depositional environment (Naji et al., 2010).

5.2.1.1 Walther's Law of Facies:

Walther's Law of facies, also known as Walter's law, states that the vertical succession of facies reflects the lateral changes in environment. That is, when a depositional environment migrates laterally, sediments of one environment come to lie over the other sediment. Vertical

stratigraphic succession is the typical example of this law. But this law is not applicable where we have unconformable boundary between lithologies (Lucia, 1995).

5.2.2 Metamorphic facies:

The concept of metamorphic facies was first introduced by Eskola (1915), he proposed its definition in 1920 i.e. some metamorphic facies is the group of rocks containing definite set of minerals. The qualitative and quantitative mineral composition in the rocks of a given facies dependent upon the bulk chemical composition of rocks. Rocks which are formed under the same temperature and pressure conditions have same facies. So, like sedimentary facies metamorphic facies dependent upon the different metamorphic conditions (Turner, 1981). Figure 5.3 shows the metamorphic facies dependent upon temperature and pressure. Figure 5.3 shows that Granulite is most stable at high temperature and low pressure but at high pressure and temperature Eclogite is most stable. Zeolite is most unstable.

5.3 Facies Analysis:

Depending upon the depositional environment and sedimentary process geologic facies vary in lithology and rock properties and they have different seismic signatures (Nanda, 2016).

Development of a facies classification scheme is a challenging interplay between capturing enough information for environmental interpretation yet remaining simple. Particularly important is the characterization of facies such that their recognition criteria relate to critical environmental thresholds such as sea level, normal wave base, and storm wave base. These physical environmental zones regulate sedimentary textures and biotic assemblages. A good understanding of paleoecology always strengthens the interpretation and such studies should be included as part of all depositional facies studies. Depositional textures in turn affect porosity-permeability in carbonates. The vertical and lateral organization of facies is an exercise essential to sequence stratigraphic interpretations (Lucia, 1995).

5.3.1 N-PHI, DT and GR cross plot:

The standard cross plot between NPHI on y-axis and RHOB on x-axis with logarithmic data from well-9, with GR as reference on z-axis is given in the figure below. For facies analysis, I selected depth between (3560-3880) for reservoirs Chorgali and Sakesar.

In the Figure 5.4 it can be clearly seen that there is an inverse relation between sonic and neutron logs. Limestone having low NPHI and high DT comparatively to shale and have low GR value. In the Figure 5.4 below, green color showing the shale, red is for lime stone and cyan for shale-limestone. This Figure 5.4 shows that our reservoir may lie between 3760 to 3840.

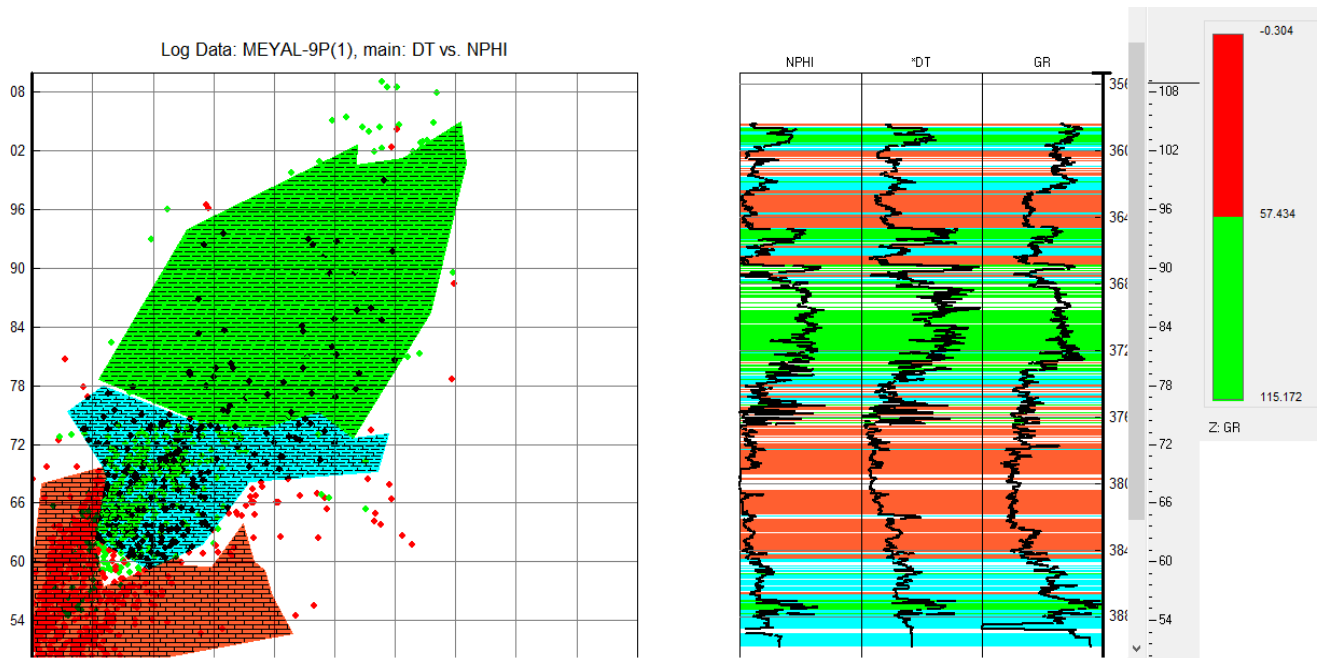


Figure 5.4: N-PHI, DT and GR cross plot

5.3.2 GR, LLD and RHOB cross plot:

There is direct relationship between LLD and RHOB for limestone reservoir i.e. due to the presence of limestone the density (RHOB) increases, while due to oil/gas resistivity (LLD) increases. Cross plot between LLD and RHOB is shown in the Figure 5.5 below. For this plot, we select logarithmic scale for LLD and linear for RHOB. Units of LLD is ohm-m and for RHOB its g/cc. depth selected for this cross plot was 3560 to 3880. RHOB is selected on X-axis and LLD on Y-axis, as a reference GR with unit's API is selected on Z-axis.

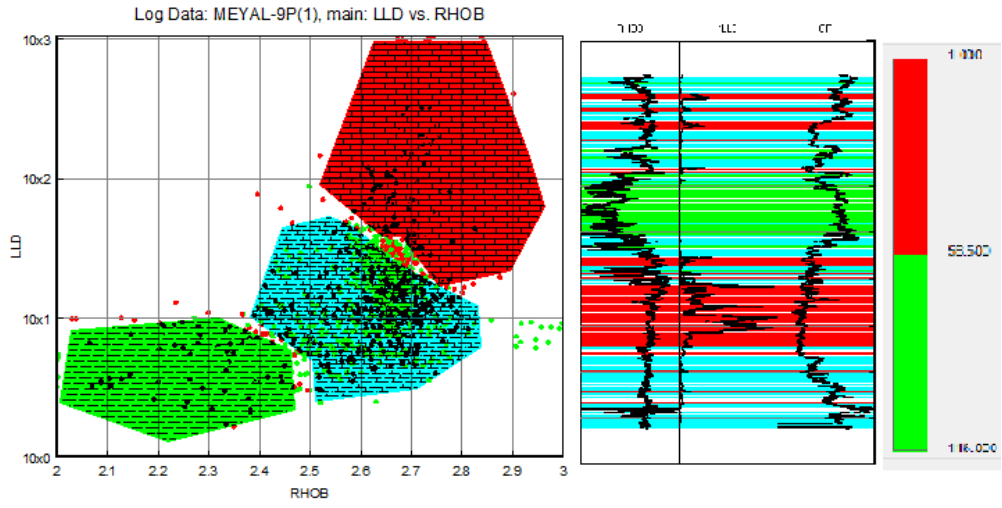


Figure 5.5: LLD Vs. RHOB

CHAPTER # 6

POST- STACK COLORED INVERSION

6.1 Introduction:

Reservoir properties as well as economic potential of field can be predicted by reservoir characterization for the development planning of reservoir and to reduce the risk and uncertainty in choosing new drilling locations a detailed study of static behavior of producing hydrocarbon is essential. For the prediction of reservoir characterization integrated analysis of well and seismic data is required. But with the conventional seismic data it's not possible due to band-limited data (Karim et al., 2016). To overcome this and to improve the interpretation of reservoir characteristics we invert the seismic band-limited data into Acoustic Impedance (AI), first at well and then generate whole AI section. In case of broad-band seismic data, the recursion formula (Oldenburg et al., 1983) is used perfectly to estimate AI with all frequencies. But seismic data contain band-limited data due to some reasons such as, band-limited nature of source wavelet, noise contamination, attenuation and absorption etc. Thus, calculating the AI from recursion formula is inappropriate missing both. To calculate AI of band-limited seismic data other method has been developed by Lancaster and Whitcombe (2000), called Colored Inversion (CL). This method is simple and fast to invert band-limited seismic data into relative impedance. In this we generate a single operator to match the average seismic spectrum which matches well log impedance spectrum (Margrave, 2016).

6.2 Inversion:

Just as forward problem evaluates theoretical data, the goal of inversion is to drive a description of earth model parameters from recorded observation. Inversion appears as to apply reverse physics to derive earth model parameters. This is done by using optimizing technique in which we define mathematical function to measures the misfit between the observed and synthetic data (Asim,S. et al., 2015) Geophysical inversion involves the mapping the Earth's sub-surface structure and properties by using measurements made on the surface on earth (Russell, 1988). With the help of inversion, we can estimate layer by layer properties from interface properties (Sinha and Mohanty, 2015). For seismic inversion, we must resolve at least three problems simultaneously.

- Non-linearity, because the solving procedure is dependent upon the solution, that is, seismic wave propagation in the inversion is a function of the current model estimate.
- Non-uniqueness due to data incompleteness.

- Instability, as a small amount of data errors may cause huge perturbations in model estimate.

6.3 Colored Inversion:

Colored inversion is different from other inversion techniques similar to seismic processing. Generally, we analyze various seismic and well log spectra to define an operator that shapes the average seismic trace spectra to that of fitted smooth curve which is representative of average AI. This defines the amplitude spectrum of required operator. For this degree phase rotation is also required, which is incorporate into operator. We assume that seismic data is zero phase. The colored inversion operator is converted to the time domain and simply applied to the seismic volume using convolution algorithm.

6.4 Convolutional Model:

The most common and basic used one-dimensional model for seismic trace is known as the convolutional model, which states that seismic trace is the convolution of seismic source (wavelet) with earth's reflectivity series plus the noise component (Russell, 1988).

$$S(t) = w(t) * r(t) + n(t), \quad (6.1) \text{ where,}$$

$s(t)$ = seismic trace in time domain, $w(t)$ = seismic wavelet in time domain, $r(t)$ = earth's reflectivity in time domain and, $n(t)$ = noise component.

This convolutional model is useful for understanding the changing in the rock properties with change in waveform changes observed in seismic data. At geological boundaries, the magnitude of change in rock properties (reflection coefficient) determines how much of wavelet's energy is reflected to the surface. Figure 6.1, shows the systematic generation of synthetic seismogram. As we can see in the Figure 6.1, for the generation of synthetic well logs and seismic data both are used. In Figure 6.1, I represented time/depth values with DT, RHOB and GR logs response of well-17, extracted wavelet, positive and negative extracted synthetics with seismic trace at well location.

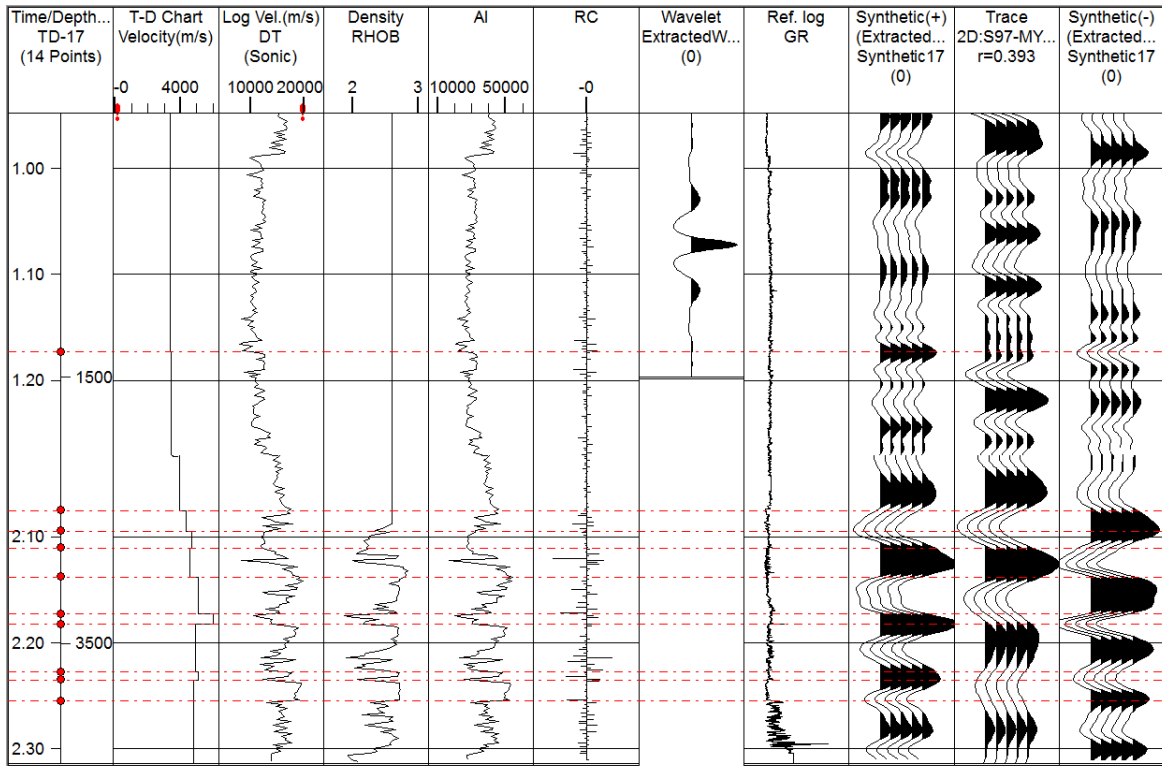


Figure 6.1: Synthetic Seismogram at well-17

6.5 Acoustic Impedance:

Acoustic Impedance (AI) is defined as the product of seismic velocity with density, which gives the basic physical property of the rocks. With the help of this we can predict the nature of rocks and change in lithologies. Seismic traces are converted into pseudo-reflection-coefficient time series by appropriate initial processing, then into acoustic impedance by inversion of time series. (Laverpne, 1975 and Lindseth, 1976).

The seismic traces are first transformed into pseudo-reflection-coefficient time series, and then converted into acoustic impedances using the recursive algorithm.

$$Z_{i+1} = Z_i \left[\frac{1+r_i}{1-r_i} \right], \quad (6.2)$$

where,

z_i = Acoustic impedance if i^{th} reflector.

r_i = Reflection coefficient of i^{th} reflector.

As low frequency is absent on seismic trace so we must add these missing frequencies. Inversion of seismic data to Acoustic Impedance (AI) is usually seen as a specialist activity.

Despite publicized benefits, inverted data are only used in a minority of cases. To help overcome this obstacle, this algorithm which is quick and easy to use, can increase the use of inversion technology. Colored inversion performs significantly better than traditional fast-track methods such as recursive inversion, and benchmarks well against unconstrained sparse-spike inversion (Becquey et al., 1979). Figure 6.2 show the general work flow for AI generation by inverting the seismic trace (data). In this Figure 6.2, for the generation of AI we use equation (6.2). the end products of inversion are density and sonic logs shown in the last two tracks.

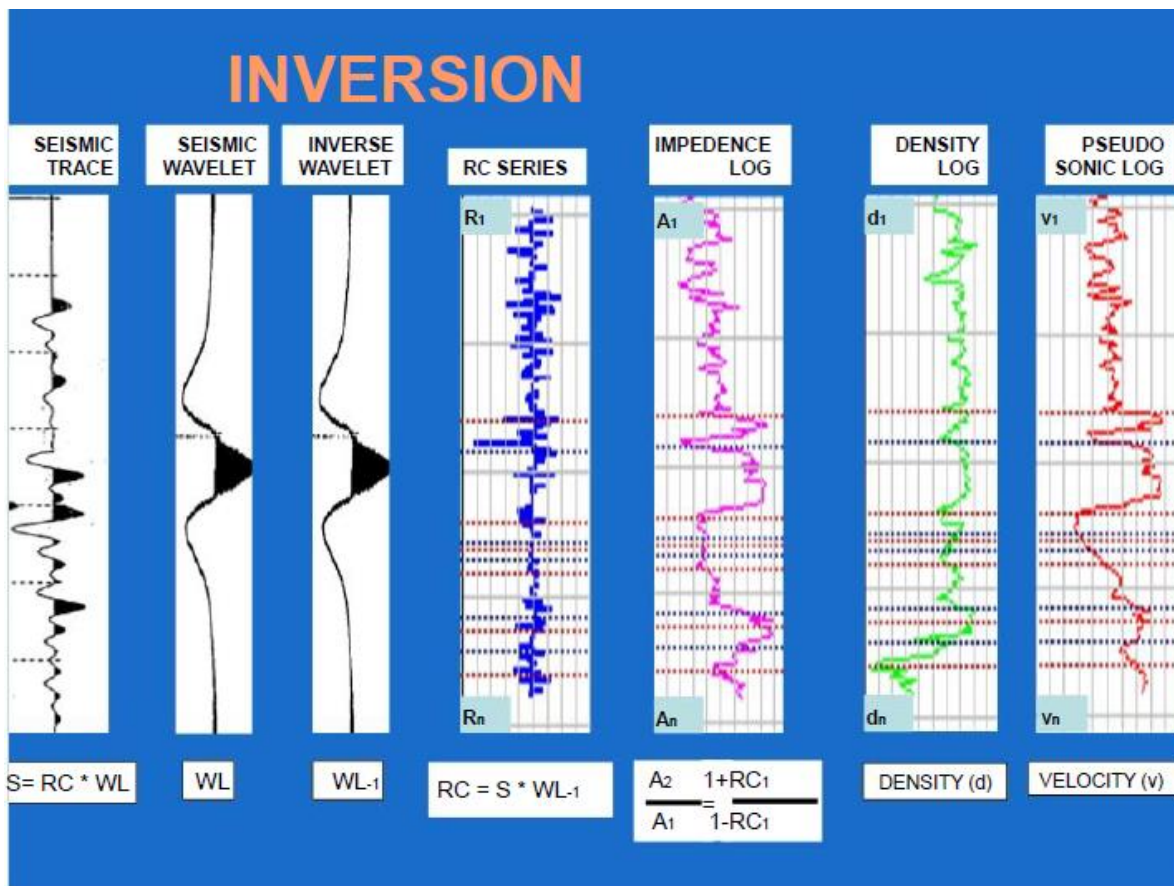


Figure 6.2: Generation of AI (Ali, 2010)

6.6 Wavelet:

Simply seismic wavelet is defined as the wave pulse approximation (mathematical function) for a seismic source contains many frequencies and is time limited (Farroqui et al., 2013). Wavelet is both time varying and complex in shape. As earth acts as natural filter which converts spike into a long band-limited wavelet. The elongation of spike is due to many factors like, unconsolidated near surface layer, instrument response and frequency and amplitude attenuation etc. Some of the effects can be compensated by deconvolution. The computation of this composite wavelet from the data provides a close approximation of the reflectivity series following the technique described by (Rice, 1962).

The seismic wavelet is the important link between seismic data and stratigraphy as well as rock properties of the subsurface. Because the character of wavelet is imprinted on seismic traces, it is important to understand its shape in order to decipher the properties of earth's interior from seismic traces.

The problem of computing the wavelet from the trace can be better understood in the frequency domain. By using formula, for amplitude spectrum we use multiplication instead of convolution. While adding the phase spectrum.

$$s(f) = w(f) \times r(f) + n(f) \quad (6.3)$$

$$\theta_s(f) = \theta_w(f) + \theta_r(f) \quad (6.4)$$

$s(f)$ = Fourier transform of $s(t)$.

$w(f)$ = Fourier transform of $w(t)$.

$r(f)$ = Fourier transform of $r(t)$.

θ = phase spectrum.

Three inverse problems are identified.

- Estimation of the wavelet when the reflection co-efficient is known.
- Estimation of reflection co-efficient or acoustic impedances when the wavelet is known.
- Simultaneous inversion for acoustic impedance of wavelet.

Figure 6.3, shows the general work flow for inversion, starting from the generation of impedance model, then convolved with extracted wavelet to generate synthetic seismogram. After that we compare this calculated and observed synthetic, if there is any error then we measure it and improve our model and convolved again. If this model best fits the observed seismic than we apply it on whole section and rock properties like porosity and lithology estimated accurately with high resolution.

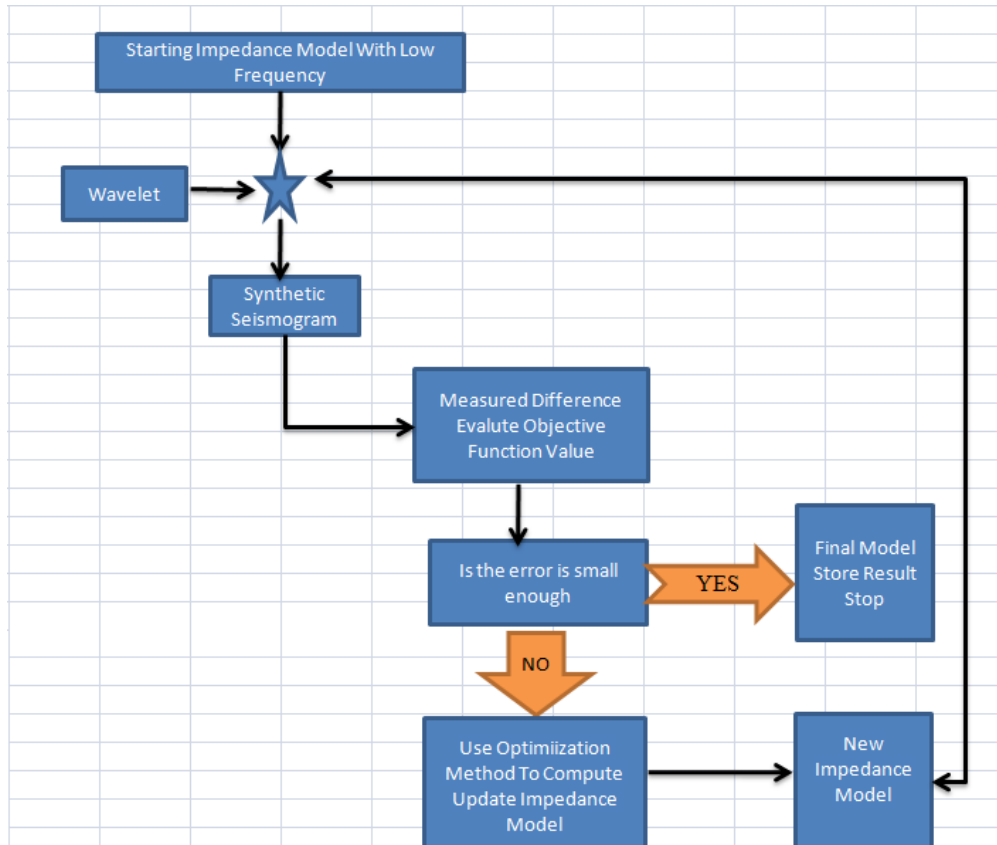


Figure 6.3: Inversion Workflow

6.7 Procedure:

Following well logs and informations are required for colored inversion in Kingdom Software.

- The velocity and density is obtained from the sonic (DT) and density (RHOB) logs respectively. By convolving we develop acoustic impedance.
- Generated acoustic impedance is cross-matched with the input reflection data.
- We derive a single optimal matching filter, convolution of this filter with the input data.

- This Empirical observation indicates that inversion can be approximated with a simple filter and that it may be valid over a sizeable region.

The phase of the operator is a constant -90° which agrees with the simplistic view of inversion being akin to integration, and the concept of a zero-phase reflection spike being transformed to a step AI interface, provided the data are zero-phase.

6.8 Wavelet Extraction:

The wavelet is shown in Figure 6.4 is extracted based on the well log data that provides the true reflectivity series (i.e. compressional wave velocity and density computed into acoustic impedance logs, which are mapped into normal incidence reflectivity series). An initial guess of wavelet is convolved with reflectivity series and synthetic normal incidence trace is generated. The difference between the observed and synthetic traced is minimized by applying different limitations. (Sen) .

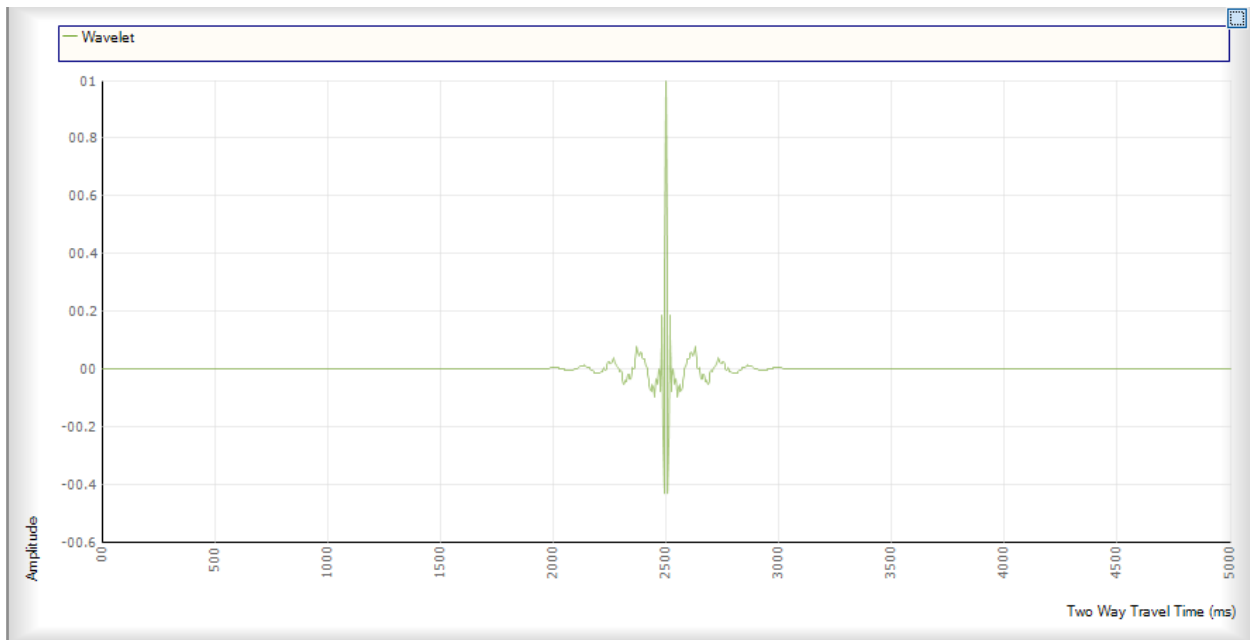


Figure 6.4: Extracted Wavelet

After obtaining a wavelet estimate, the wavelet is used to design an inverse operator to zero-phase deconvolve the seismic. The deconvolution may be a de-phase only or a full-inverse procedure to correct both the phase and the amplitude spectra.

6.9 Estimation of Impedence:

The colored inversion method is based on a special filtering technique. In the inversion amplitude spectrum of well log is compared with seismic data. Figure 6.5 showing the impedance spectrum with fitted line estimated after removing source wavelet, noise and multiples should be removed (Ghosh 2000). To remove the mismatch between well spectrum and seismic spectrum we develop an operator. This operator is then applied to the whole seismic data (Lancaster and Whitcombe 2000). To compute the operator a cross plot between amplitude and logarithm of frequency is made. A linear fit is shown in the Figure 6.5, is performed to calculate an exponential function which serves as a shaping filter (Walden and Hosken 1985, Velzeboer 1981). This filter transforms the seismic trace into an assumed equivalent acoustic impedance. We also assume that the seismic inputcube is zero-phase, which is hardly ever the case. Now our approach is to convolve the extracted wavelet with acoustic impedance (reflectivity series). The acoustic impedance is also computed from well log data as described early.

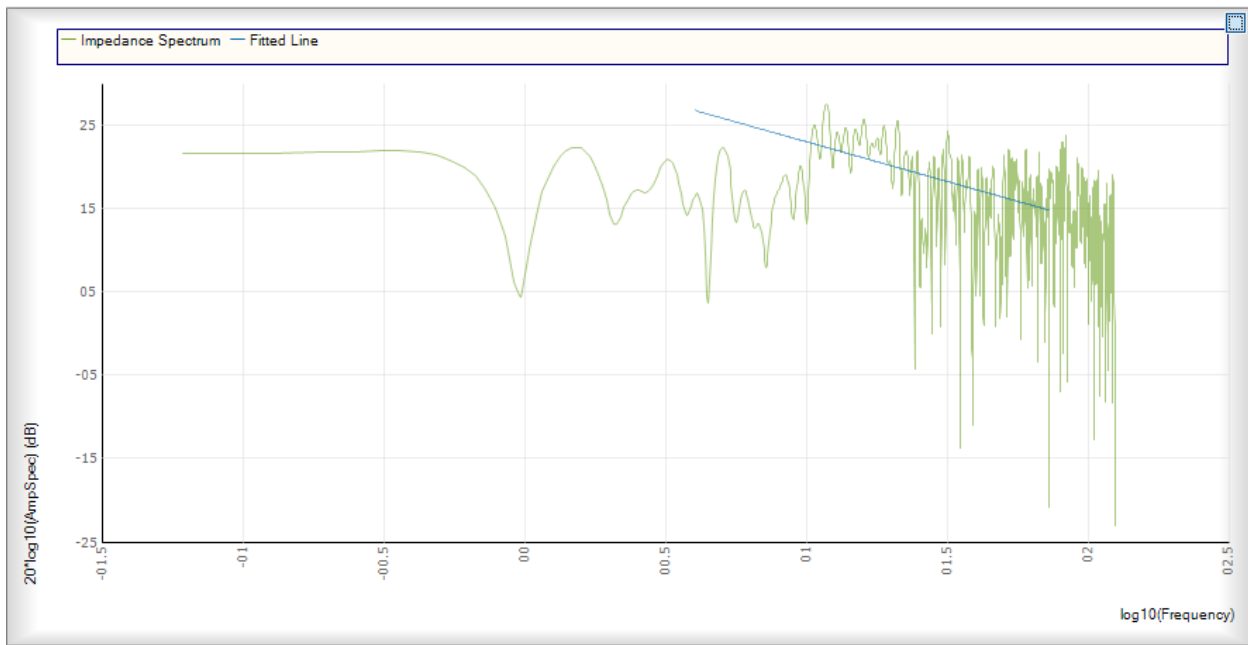


Figure 6.5: Impedance Spectrum with Fitted Line

6.10 Butterworth Filter:

The Butterworth filter is a type of signal processing filter designed to have as flat a frequency response as possible in the pass band. It is also referred to as a maximally flat

magnitude filter. It was first described in 1930 by the British engineer and physicist Stephen Butterworth in his paper entitled “On the Theory of Filter Amplifiers”.

An ideal electrical filter should not only completely reject the unwanted frequencies but should also have uniform sensitivity for the wanted frequencies. This filter is used here for convolution of the wavelet and reflectivity series for formulation of seismogram. The Butterworth filter is shown in Figure 6.6.

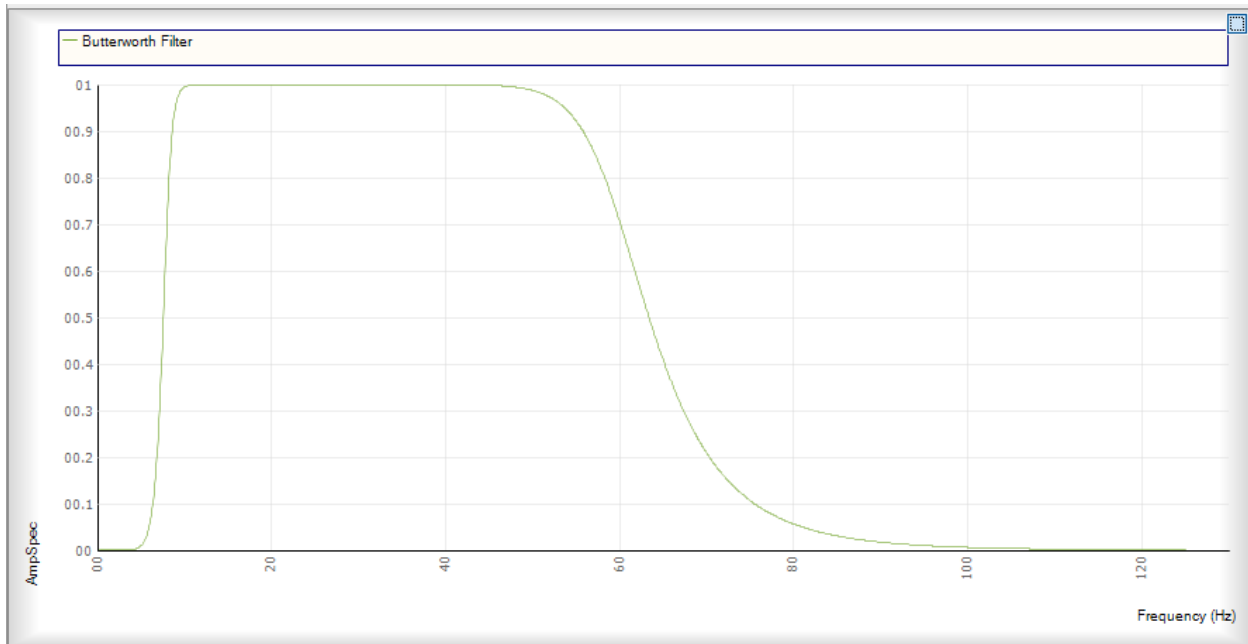


Figure 6.6: Butterworth Filter

An operator is designed bringing the seismic amplitudes in correspondence with those seen in the well. This operator is subsequently applied to the whole seismic cube (Lancaster and Whitcombe, 2000). After the process of convolution is performed we get the seismogram (operator). There is a vast difference between the seismogram of our desire and the seismogram we obtained from the convolution.

There are two spectrums shown in Figure 6.7 both are of different colors. The blue color shows the spectrum obtained from convolution of wavelet and acoustic impedance and the spectrum in blue color shows a desired spectrum. Now we need to obtain a spectrum of our desire for this purpose we must convolve this spectrum with another spectrum known as shaping spectrum

which is obtained by applying Fourier transformation on desired spectrum. The shaping spectrum is shown in Figure 6.8.

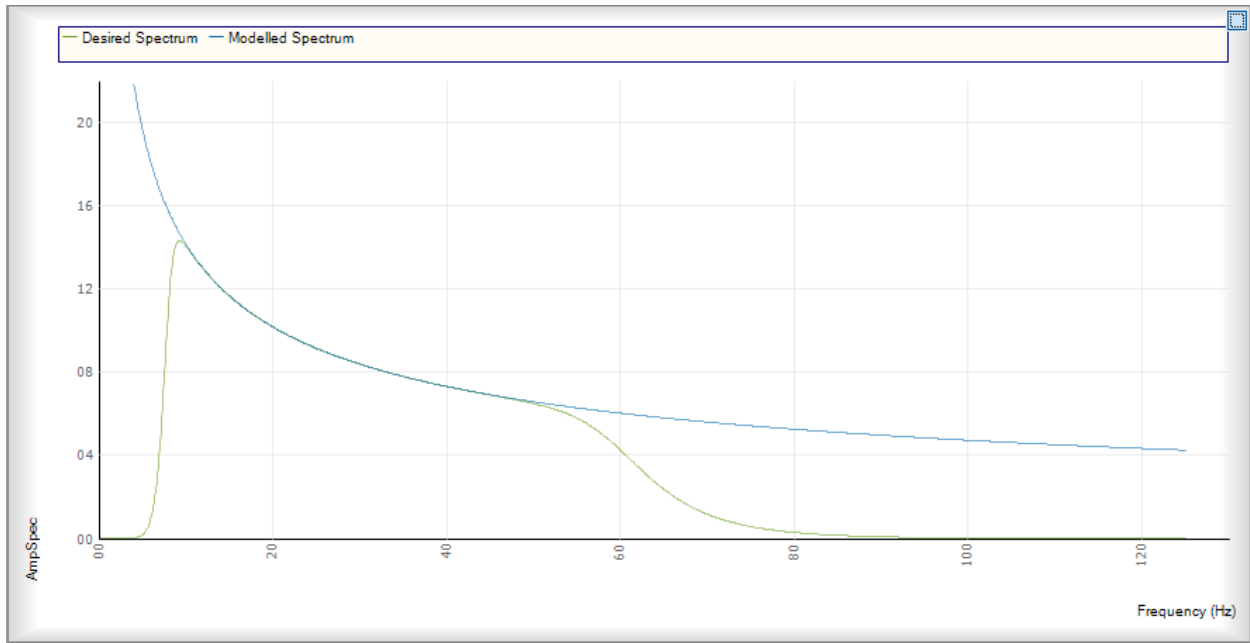


Figure 6.7: Desired and Modeled Spectrum

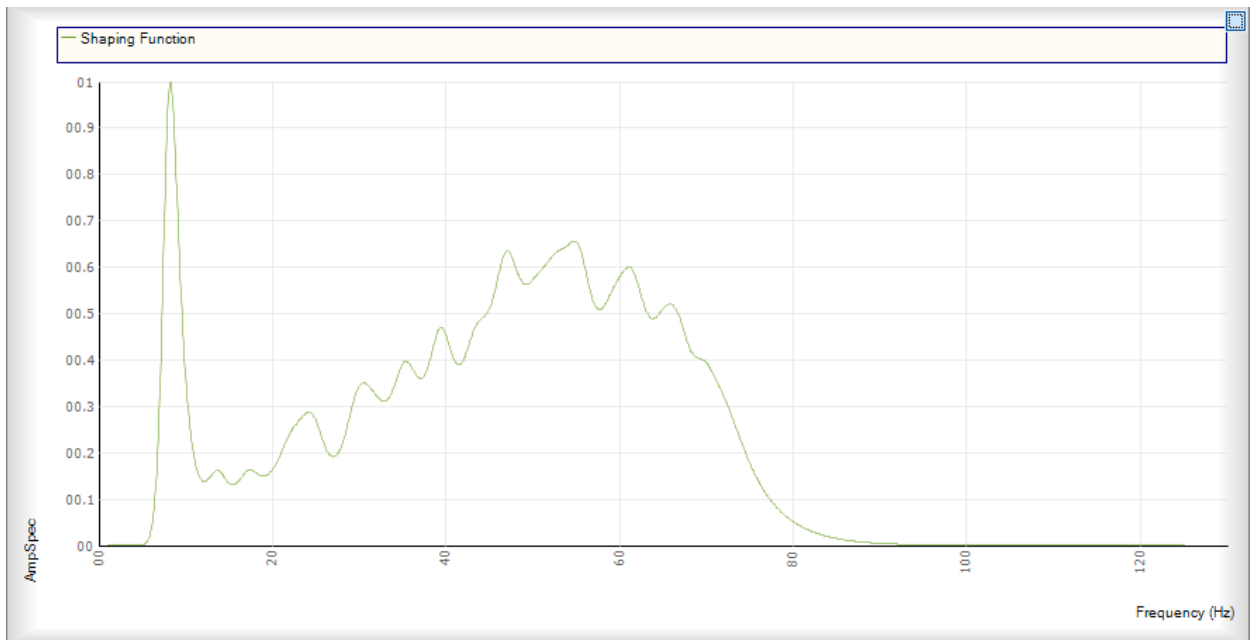


Figure 6.8: Shaping Spectrum

A cross plot is made between the amplitude and the logarithm of the frequency to compute the operator. A linear fit is performed to calculate an exponential function and this serves as a shaping filter (Walden and Hosken 1985, Velzeboer 1981).

The figure 6.9 shows us the shaped seismic spectrum and desired seismic spectrum.

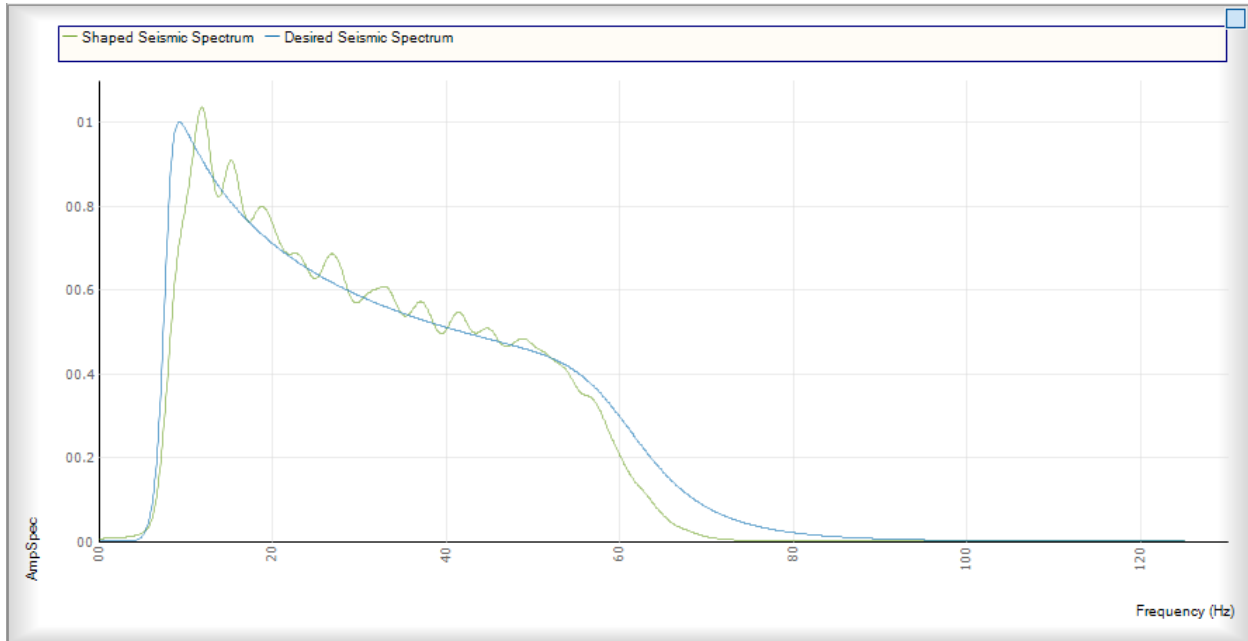


Figure 6.9: Convolution of shaped seismic spectrum and desired spectrum.

A seismogram for specific window (as values of acoustic impedance is obtained from well data) is developed now we develop a seismogram to invert whole section. For this purpose, we convolve desired spectrum with seismic mean spectrum. After convolving seismogram with seismic mean spectrum we are able to apply it on whole seismic section. The figure 6.10 shows seismic mean spectrum and desired spectrum.

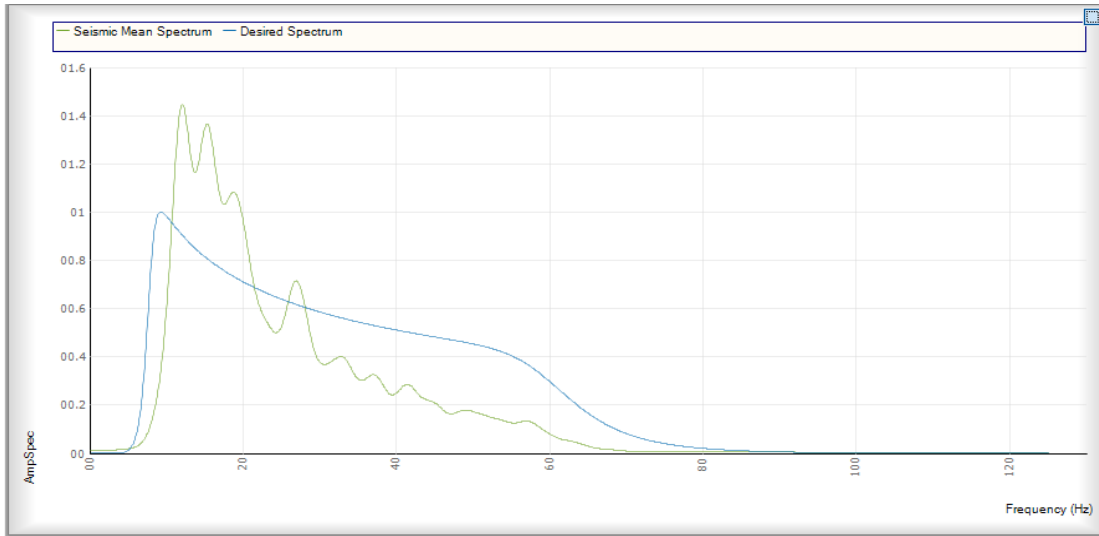


Figure 6.10: convolution of seismic mean spectrum and desired spectrum

After completion of the process of generating synthetic seismogram, the section is inverted an acoustic impedance is shown on section instead of amplitude as shown in figure (6.11).

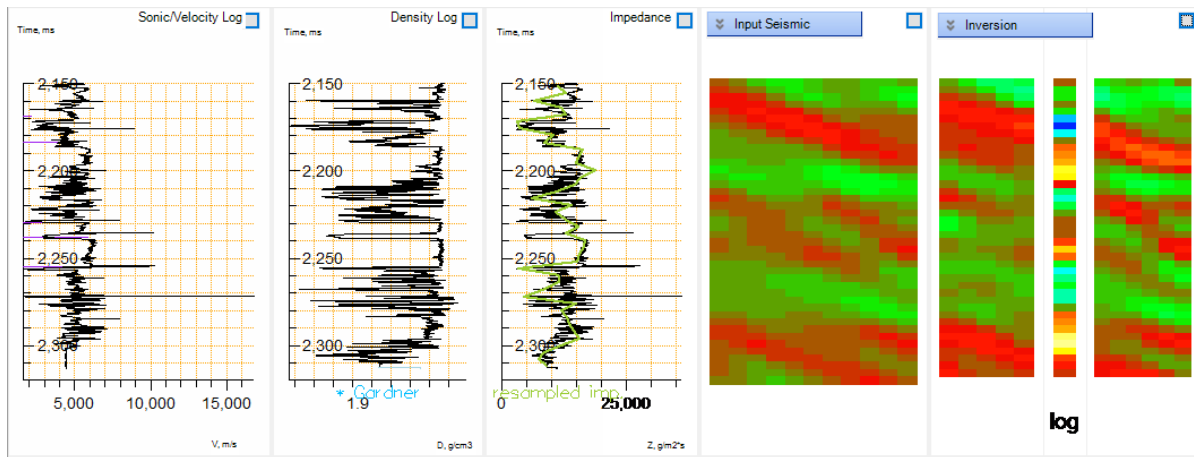


Figure 6.11 Input Seismic Section and inverted section with logs

From the Figure 6.11, this window displays sonic log and density logs. These logs are used to compute the acoustic impedance. If values of density log are missing, then Gardner equation is used to estimate these densities. This equation is very popular in petroleum exploration because it can provide information about the lithology from interval velocities obtained from data these values are calibrated from sonic and density well log information but in the absence of these, Gardner's constants are a good approximation for density. At the right

corner of the window input seismic section is shown on left side and inverted section is shown on the right-hand side. The inverted section is shown on the both sides of logs sides of the well the log is inverted to invert the seismic section.

The zoomed picture of inverted section is shown in the Figure (6.12) given below, with the inverted log and inverted seismic section.

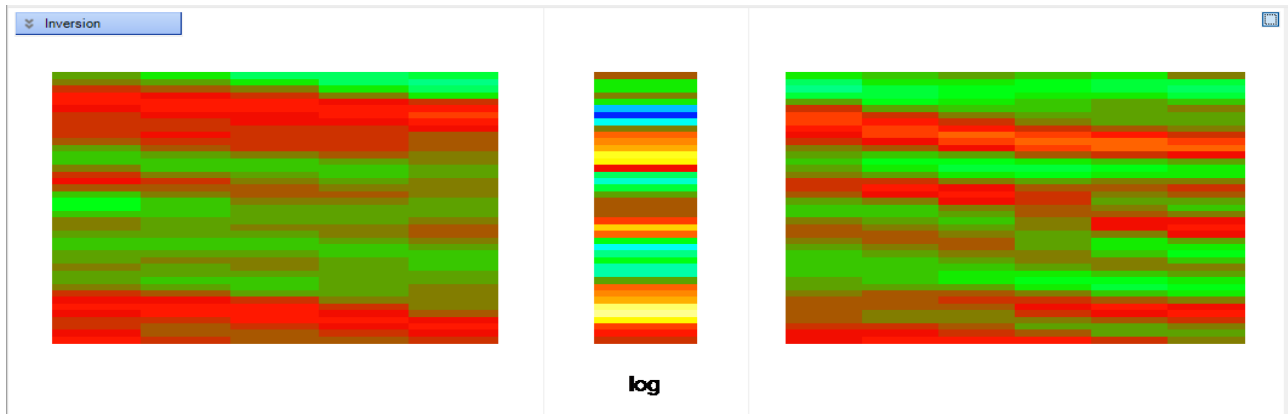


Figure 6.12: Inverted section with inverted logs

Now the inversion is applied to the whole section which is shown in Figure 6.13, with well-17 location and chorgali and sakassar are marked. On the right side, there is a relative scale.

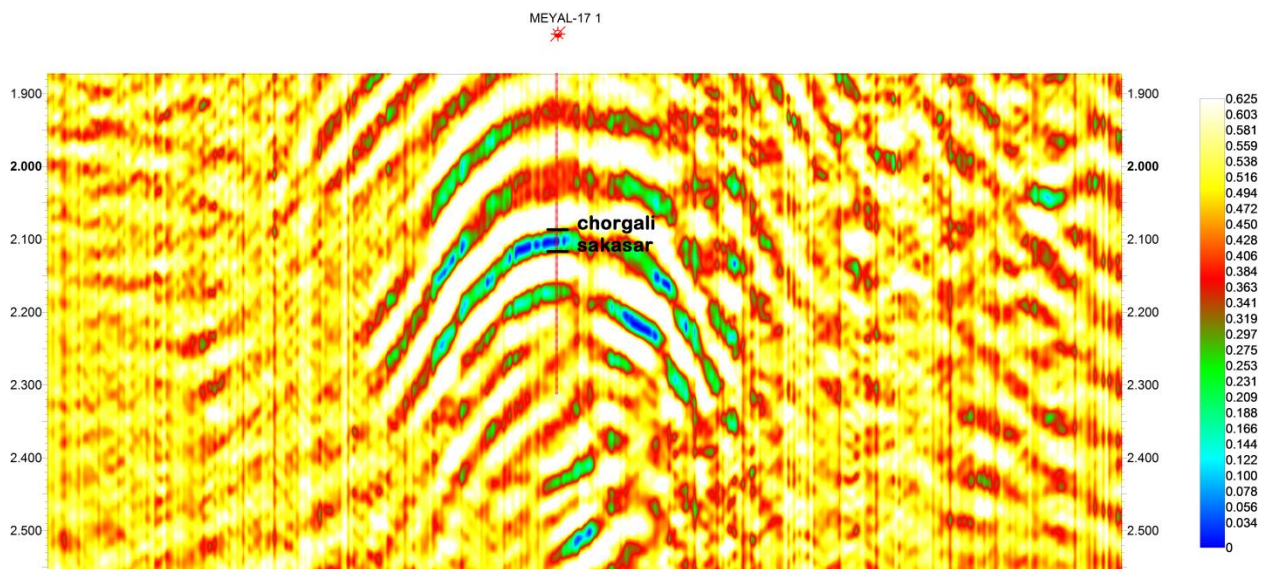


Figure 6.13: Inverted Seismic Section

6.11 Interpretation of Inverted Section:

After convolution of seismogram with mean spectrum an inverted seismic section is generated as shown in the above Figure (6.13). The inverted section can be interpreted by using color bar. The white to yellow color shows high values of acoustic impedance and blue to green color shows low impedance.

The hydrocarbons accumulation is associated with low acoustic impedance. The given inverted section is shown with T-D chart and it shows Formations as well. The Formation circled in figure (6.12) is Chorgali, which yields a response of low acoustic impedance it is related to presence of hydrocarbon accumulation it is also confirmed from Petrophysical results.

The Chorgali is interpreted as main producing reservoir in Meyal area. Because results obtained from seismic inversion shows low values of impedance with pop-up structure, these both conditions give indication for presence of hydrocarbons. The zoomed view in Figure 6.14 also confirms our results.

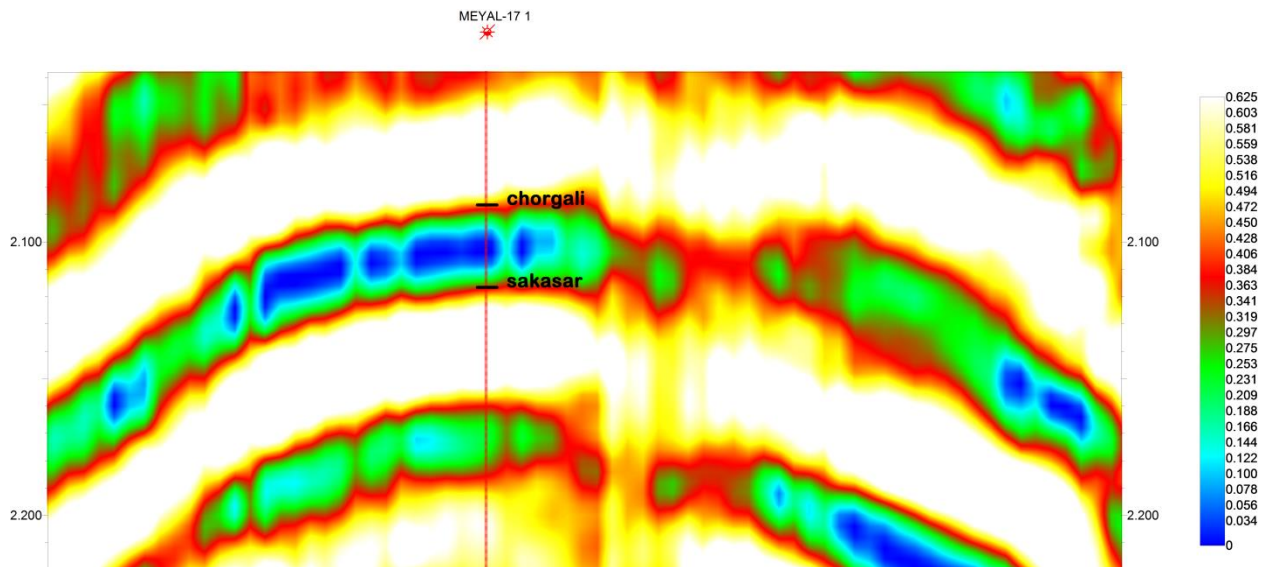


Figure 6.14: Zoomed view of inverted section showing chorgali

Conclusions:

- Time and Depth contour maps of Chorgali and Sakesar Formation help us to confirm the presence of pop-up structures in my study area. Surface contour maps of Chorgali and Sakesar Formations give the real shape of sub-surface structure, which is anticlinal, bonded with thrust faulting. These fault bounded pop-up structures act as the structural traps in the Meyal area, which is best for hydrocarbon accumulation. This shows that the study area is dominated by compressional tectonic forces.
- The pseudo-synthetic trace is generated via well log confirms the marking of right seismic sections.
- Based on time and depth contour maps various leading zones are marked ut for the exploration we have use dense seismic data i.e. more number of seismic lines. But these zones partially confirmed by petrophysics, facies and inversion. These leads are marked on Chorgali and Sakessar.
- The seismic attribute analysis of given 2D data confirms the interpretation also for the detection of hydrocarbon, rate of sedimentation and its preservation at some locations but not give any reliable location to identify hydrocarbons due to limitation of data control.
- Petrophysical analysis and Facies modeling of the reservoir of the well MYL-09, show fine hydrocarbon potential and its concluded results show that Chorgali Formation is more hydrocarbon bearing than the Sakessar. These techniques also help to verify our interpretation results.
- With the help of Colored Inversion, we improve the resolution. We compare the synthetic with seismic to confirm our prospect zone. Leads are confirmed by inversion when we apply it on full section.

References

- Aamir, M., & Siddiqui, M. M. (2006). Interpretation and visualization of thrust sheets in a triangle zone in eastern Potwar, Pakistan. *The Leading Edge*, 25(1), 24-37.
- Ahmed, K. A., Man, H. Q., & Zeb, Y. (1926). Seismic facies modelling of Potwar Basin using seismic and well log data. *Geosciences*, 2(6), 192-211.
- Anstey, N. A. (2013). *Seismic interpretation: the physical aspects*. Springer Science & Business Media.
- Asim, S., Zhu, P., Qureshi, S. N., & Naseer, M. T. (2015). A case study of Precambrian to Eocene sediments' hydrocarbon potential assessment in Central Indus Basin of Pakistan. *Arabian Journal of Geosciences*, 8(12), 10339-10357.
- Asquith, G. B., Krygowski, D., & Gibson, C. R. (2004). *Basic well log analysis*(Vol. 16). Tulsa: American association of petroleum geologists.
- Becquey, M., Lavergne, M., & Willm, C. (1979). Acoustic impedance logs computed from seismic traces. *Geophysics*, 44(9), 1485-1501.
- Becquey, M., Lavergne, M., & Willm, C. (1979). Acoustic impedance logs computed from seismic traces. *Geophysics*, 44(9), 1485-1501.
- Chatterjee, R., Gupta, S. D., & Farroqui, M. Y. (2013). Reservoir identification using full stack seismic inversion technique: A case study from Cambay basin oilfields, India. *Journal of Petroleum Science and Engineering*, 109, 87-95.
- Coffeen, J. A. (1986). *Seismic exploration fundamentals*.
- *Coloured, Deterministic & Stochastic Inversion*
- Dvorkin, Jack, et al. "Elasticity of marine sediments: Rock physics modeling." *Geophysical research letters* 26.12 (1999): 1781-1784.
- Eaton, David W., Bernd Milkereit, and Matthew Salisbury. "Seismic methods for deep mineral exploration: Mature technologies adapted to new targets." *The Leading Edge* 22.6 (2003): 580-585.
- Fatemi, A. M. (1984). Shareholder benefits from corporate international diversification. *The Journal of Finance*, 39(5), 1325-1344.
- Gadallah, M. R., & Fisher, R. (2009). Data Acquisition–Seismic data Processing. *Exploration Geophysics*. Springer-Verlag Berlin Heidelberg. DOI, 10, 978-3.

- Gauthier, B. D. M., & Lake, S. D. (1993). Probabilistic modeling of faults below the limit of seismic resolution in Pelican Field, North Sea, offshore United Kingdom. *AAPG Bulletin*, 77(5), 761-777.
- Gee, E. R. (1934). The Saline Series of north-western India. *Current Science*, 2(12), 460-463.
- Hallam, A. (1975). Alfred Wegener and the hypothesis of continental drift. *Scientific American*, 232(2), 88-97.
- Handwerger, D. A., Cooper, A. K., O'Brien, P. E., Williams, T., Barr, S. R., Dunbar, R. B., ... & Jarrard, R. D. (2004). Synthetic seismograms linking ODP sites to seismic profiles, continental rise and shelf of Prydz Bay, Antarctica. *Cooper, AK, O'Brien, PE, and Richter, C., et al., Proceedings of the Ocean Drilling Program, Scientific Results*, 188, 1-28.
- Hasany, S. T., & Saleem, U. (2012). An integrated subsurface geological and engineering study of Meyal field, Potwar plateau, Pakistan. *Search and Discovery Article*, 20151, 1-41.
- Kadri, I. B. (1995). *Petroleum geology of Pakistan*. Pakistan Petroleum Limited.
- Karim, S. U., Islam, M. S., Hossain, M. M., & Islam, M. A. (2016). Seismic Reservoir Characterization Using Model Based Post-stack Seismic Inversion: In Case of Fenchuganj Gas Field, Bangladesh. *Journal of the Japan Petroleum Institute*, 59(6), 283-292.
- Kazmi, A. H., & Jan, M. Q. (1997). *Geology and tectonics of Pakistan*. Graphic publishers.
- Kearey, P., Brooks, M., & Hill, I. (2013). *An introduction to geophysical exploration*. John Wiley & Sons.
- Kearey, P., Brooks, M., & Hill, I. (2013). *An introduction to geophysical exploration*. John Wiley & Sons.
- Lancaster, S., & Whitcombe, D. (2000). Fast-track 'coloured' inversion. In *SEG Technical Program Expanded Abstracts 2000* (pp. 1572-1575). Society of Exploration Geophysicists.
- Law, B. E. (1998). *Memoir 70, Chapter 14: Abnormally High Formation Pressures, Potwar Plateau, Pakistan*.

- Lindseth, R. O. (1979). Synthetic sonic logs—A process for stratigraphic interpretation. *Geophysics*, 44(1), 3-26.
- Lukic, Ivana, Davor Barac, and Danijela Zovko. "Seismic Refraction Method." International Balkans Conference on Challenges of Civil Engineering, 2013.
- McQuillin, R., Bacon, M., & Barclay, W. (1984). An introduction to seismic interpretation-Reflection seismics in petroleum exploration.
- Moore, R. C. (1949). Meaning of facies. *Geological Society of America Memoirs*, 39, 1-34.
- Mutti, E., & Ricci Lucchi, F. (1978). Turbidites of the northern Apennines: introduction to facies analysis. *International geology review*, 20(2), 125-166.
- Nanda, N. C. (2016). Seismic data interpretation and evaluation for hydrocarbon exploration and production: A practitioner's guide. Springer.
- Ousaka J, O'Donovan A (2000) Exposing the 4D seismic time-lapse signal imbedded the Foinaven active reservoir management project, OTC paper 12097
- Partyka, Greg, James Gridley, and John Lopez. "Interpretational applications of spectral decomposition in reservoir characterization." *The Leading Edge* 18.3 (1999): 353-360.
- Pennock, E. S., Lillie, R. J., Zaman, A. S. H., & Yousaf, M. (1989). Structural interpretation of seismic reflection data from eastern Salt Range and Potwar Plateau, Pakistan. *AAPG Bulletin*, 73(7), 841-857.
- Russell, B. H. (1988). Introduction to seismic inversion methods. Society of Exploration Geophysicists.
- Serra, K. V. (1988). Well testing for solution gas drive reservoirs. Tulsa Univ., OK (USA).
- Shami, B. A., & Baig, M. S. (2002, November). Geomodeling for enhancement of hydrocarbon potential of Joya Mair Field (Potwar) Pakistan. In PAPG-SPE Annual Technical Conference, Islamabad (pp. 124-145).
- Sheriff, R.E., (1999), "Encyclopedia Dictionary of Exploration Geophysics", Society of Exploration Geophysicists, Tulsa, Oklahoma.

- Sinha, B., & Mohanty, P. R. (2015). Post stack inversion for reservoir characterization of KG Basin associated with gas hydrate prospects. *Journal of Indian Geophysical Union*, 19(2), 200-204.
- Sloss, L. L., Krumbein, W. C., & Dapples, E. C. (1949). Integrated facies analysis. *Geological Society of America Memoirs*, 39, 91-124.
- Taner, M. T. (2001). Seismic attributes. *CSEG recorder*, 26(7), 48-56.
- Velzeboer, C. J. (1981). The theoretical seismic reflection response of sedimentary sequences. *Geophysics*, 46(6), 843-853.
- Walden, A. T., & Hosken, J. W. J. (1985). An investigation of the spectral properties of primary reflection coefficients. *Geophysical Prospecting*, 33(3), 400-435.